NATIONAL ADVISORY COMMITTEE FOR AERONAUTICS

TECHNICAL NOTE 2612

STRESS PROBLEMS IN PRESSURIZED CABINS

By W. Flügge

Stanford University

Washington
February 1952

1C

NATIONAL ADVISORY COMMITTEE FOR AERONAUTICS

TECHNICAL NOTE 2612

STRESS PROBLEMS IN PRESSURIZED CABINS

By W. Flügge

SUMMARY

The report presents information on the stress problems in the analysis of pressurized cabins of high-altitude aircraft not met with in other fields of stress analysis relating to aircraft. The material may be roughly divided into shell problems and plate problems, the former being concerned with the curved walls of the cabin or pressure vessel and the latter being concerned with small rectangular panels of its walls, framed by stiffeners, but not necessarily plane.

INTRODUCTION

The analysis of pressurized cabins of high-altitude aircraft presents particular stress problems not usually met with in other fields of stress analysis relating to aircraft. It is the purpose of the present report to gather information on these problems and to make it easily accessible to aircraft engineers. Some of the work in this field is presented in references 1 to 10.

This report contains a choice of subjects taken from the theory of plates and shells which is expected to be useful for the designer of pressurized airplane cabins or similar lightweight pressure vessels. This material may be roughly divided into shell problems and plate problems, the former being concerned with the curved walls of the cabin or pressure vessel and the latter, with small rectangular panels of its walls, framed by stiffeners, but not necessarily plane.

As far as shell problems are concerned, some use has been made of a manuscript for a book on "Stresses in Shells," which the author is preparing. (See reference 3.) The prospect that this book will be available some time in 1952 makes it possible to discuss in the present report several problems which are too complex to explain here in all their mathematical details.

The pressurized cabin is a rather new element in the airplane structure and will, in all probability, undergo future development. In view of this situation, no attempt has been made to present anything like a textbook on the subject giving time-tested methods for solving

various problems, but rather an attempt has been made to show the general lines of thought which have proved to be useful and to give suggestions for their application.

This investigation was carried out at Stanford University under the sponsorship and with the financial assistance of the National Advisory Committee for Aeronautics.

SYMBOLS

x,y,z	rectangular coordinates
ϕ,θ	angular coordinates
u,v,w	displacements
a	radius of cylinder or sphere
a,b	sides of rectangle; axes of ellipse or ellipsoid
l	span of beam
t	thickness of plate or shell
p	pressure difference between interior and exterior of cabin
X,Y,Z	distributed load on shells (force per unit area of middle surface), in directions ϕ, θ, and radial
N_ϕ,N_θ,N_x	normal forces in shells (force per unit length of section), in direction ϕ, θ, or x
M_x,M_y,M_ϕ	bending moment in plates and shells (moment per unit length of section)
M_{xy}	twisting moment in plates (moment per unit length of section)
σ	normal stress
τ	shear stress
E	elastic modulus
ν	Poisson's ratio

SHELL PROBLEMS

Cylindrical Shell

Circular cylinder.- The fuselage of a high-altitude passenger plane is usually of circular cross section and is, for most of its length, almost cylindrical. Some useful information regarding its strength may be found, therefore, when a circular cylinder closed at both ends by some kind of bulkhead which permits the air pressure inside to be greater than that outside (fig. 1) is considered. The pressure difference will be called p.

For a homogeneous shell of thickness t the stresses produced by this pressure are given by the well-known boiler formulas for hoop stress σ_ϕ and axial stress σ_x:

$$\left.\begin{aligned} \sigma_\phi &= pa/t \\ \sigma_x &= pa/2t \end{aligned}\right\} \qquad (1)$$

The shell of a pressure cabin is reinforced by rings and stringers, which participate in carrying the load. The stringers will always be spaced closely enough to make the distribution of the longitudinal stress on the skin between them practically uniform. With the rings this may be different. The limiting case, that is, that they too are closely spaced, will be considered here.

In finding the stresses, start from the internal forces per unit length of section acting in the shell. When a slice of length $\Delta x = 1$ is cut out of the shell (fig. 2), the hoop force

$$N_\phi = pa$$

is found, and when the force $p\pi a^2$ acting on each bulkhead is distributed over the circumference $2\pi a$ of the cylinder, the longitudinal force

$$N_x = \frac{1}{2} pa$$

transmitted by the unit length of a section right across the shell is found.

If the shell has no stiffeners, the stresses σ_ϕ and σ_x are found by dividing N_ϕ and N_x by the wall thickness t, which, of course, results in the boiler formulas (1). In the cabin shell are rings of cross section A_R at distance l from each other and stringers of cross section A_L at an angular distance δ (see fig. 3). If these areas are distributed over the cross section of the skin, the effective thicknesses

$$\left.\begin{aligned} t_\phi &= t + \frac{A_R}{l} \\ t_x &= t + \frac{A_L}{a\delta} \end{aligned}\right\} \qquad (2)$$

are introduced; however, the stresses σ_ϕ and σ_x are not simply the quotients N_ϕ/t_ϕ and N_x/t_x (see, e.g., reference 1). The reason for this is apparent when one considers the fact that the skin is in a two-dimensional state of stress and therefore for the same strain its stress is different from that in the stiffeners.

Let the stresses in the skin be σ_ϕ and σ_x as before, in the stringers, σ_L, and in the rings, σ_R. Then Hooke's law will yield the following relations for the hoop strain ϵ_ϕ and the longitudinal strain ϵ_x:

$$\begin{aligned} E\epsilon_\phi &= \sigma_\phi - \nu\sigma_x \\ &= \sigma_R \end{aligned} \qquad (3a)$$

$$\begin{aligned} E\epsilon_x &= \sigma_x - \nu\sigma_\phi \\ &= \sigma_L \end{aligned} \qquad (3b)$$

E being Young's modulus and ν Poisson's ratio.

On the other hand, the definition of the internal forces is:

$$\left.\begin{aligned} N_\phi &= t\sigma_\phi + \frac{A_R}{l}\sigma_R \\ N_x &= t\sigma_x + \frac{A_L}{a\delta}\sigma_L \end{aligned}\right\} \qquad (4)$$

Solving the four equations (3) and (4) for the stresses,

$$\sigma_\phi = \frac{t_x N_\phi + \nu(t_\phi - t)N_x}{(1 - \nu^2)t_\phi t_x + \nu^2 t(t_\phi + t_x - t)}$$

$$= \frac{pa}{2} \frac{2t_x + \nu(t_\phi - t)}{(1 - \nu^2)t_\phi t_x + \nu^2 t(t_\phi + t_x - t)} \tag{5a}$$

$$\sigma_R = \frac{\left[(1 - \nu^2)t_x + \nu^2 t\right]N_\phi - \nu t N_x}{(1 - \nu^2)t_\phi t_x + \nu^2 t(t_\phi + t_x - t)}$$

$$= \frac{pa}{2} \frac{2(1 - \nu^2)t_x - \nu(1 - 2\nu)t}{(1 - \nu^2)t_\phi t_x + \nu^2 t(t_\phi + t_x - t)} \tag{5b}$$

$$\sigma_x = \frac{t_\phi N_x + \nu(t_x - t)N_\phi}{(1 - \nu^2)t_\phi t_x + \nu^2 t(t_\phi + t_x - t)}$$

$$= \frac{pa}{2} \frac{t_\phi + 2\nu(t_x - t)}{(1 - \nu^2)t_\phi t_x + \nu^2 t(t_\phi + t_x - t)} \tag{5c}$$

$$\sigma_L = \frac{\left[(1 - \nu^2)t_\phi + \nu^2 t\right]N_x - \nu t N_\phi}{(1 - \nu^2)t_\phi t_x + \nu^2 t(t_\phi + t_x - t)}$$

$$= \frac{pa}{2} \frac{(1 - \nu^2)t_\phi - \nu(2 - \nu)t}{(1 - \nu^2)t_\phi t_x + \nu^2 t(t_\phi + t_x - t)} \tag{5d}$$

When the rings are far apart, these formulas are no longer applicable. The problem must then be split, with the shell without rings considered first and the influence of the rings introduced afterward (see section entitled "Interaction between Shell and Rings"). When there are no rings $t_\phi = t$, and the formulas are simplified considerably:

$$\sigma_\phi = \frac{pa}{t} \tag{6a}$$

$$\sigma_x = \frac{pa(1 - 2\nu)}{2t_x} + \frac{\nu pa}{t} \tag{6b}$$

$$\sigma_L = \frac{(1 - 2\nu)pa}{2t_x} \tag{6c}$$

It appears that σ_L is always smaller by a factor $1 - 2\nu$ than it would be if it were obtained by simply distributing N_x over the whole section. For the skin stress σ_x the factor depends on the ratio $A_L/a\delta t$, and if one writes

$$\sigma_x = k \frac{pa}{2t_x}$$

the factor k will be as shown in figure 4. For $A_L/a\delta t = 0$ the boiler formulas are valid, and $\sigma_x = 0.5\sigma_\phi$. For $A_L/a\delta t = 1.0$, the diagram shows $\sigma_x = 0.4\sigma_\phi$. The difference between these two values of σ_x is small, but both are much less than the hoop stress. This is very desirable since the over-all bending of the fuselage due to air forces acting on the control surfaces produces additional stresses σ_x which must be superimposed on the stress σ_x due to cabin pressure.

Since the stringers take an important share of the axial load, it is not good practice to interrupt them at the rings. Care should be taken to insure that the forces carried by the stringers can go straight through from one bulkhead to the other, or to the end of the cabin shell.

Double cylinders.- The circular cross section is certainly the best one, both for aerodynamic and structural reasons. However, it has some practical disadvantages when used as a passenger cabin. Most serious

is the fact that a horizontal floor must necessarily be built in, requiring additional weight and leaving beneath it space which is not easily used.

This situation is improved by a cross section which, with some exaggeration, is shown in figure 5. It consists of parts of two circles and a straight horizontal tie between them.

Begin with a discussion of the weight of this structure. Under the action of an internal pressure p the hoop stresses in the upper cylinder $\sigma_{\phi 1}$ and in the lower cylinder $\sigma_{\phi 2}$ will be:

$$\sigma_{\phi 1} = pa_1/t_1$$

$$\sigma_{\phi 2} = pa_2/t_2$$

The stress in the tie follows from the equilibrium at its ends (fig. 6):

$$\sigma_3 t_3 = \sigma_{\phi 1} t_1 \cos \alpha_1 + \sigma_{\phi 2} t_2 \cos \alpha_2$$

$$= p\left(a_1 \cos \alpha_1 + a_2 \cos \alpha_2\right)$$

If t_1, t_2, and t_3 are chosen such that the three stresses are all equal to the same value σ given by the allowable stress in the material,

$$t_1 = \frac{p}{\sigma} a_1$$

$$t_2 = \frac{p}{\sigma} a_2$$

$$t_3 = \frac{p}{\sigma}\left(a_1 \cos \alpha_1 + a_2 \cos \alpha_2\right)$$

The material invested in the structure is given by the area A_m of its metallic cross section. The two circles contribute to it

$$2t_1a_1(\pi - \alpha_1) + 2t_2a_2(\pi - \alpha_2) = \frac{p}{\sigma}\left[2a_1^2(\pi - \alpha_1) + 2a_2^2(\pi - \alpha_2)\right]$$

and the tie contributes

$$2t_3c = 2\,\frac{p}{\sigma}(a_1 \cos \alpha_1 + a_2 \cos \alpha_2)c$$

Now

$$c = a_1 \sin \alpha_1$$

$$= a_2 \sin \alpha_2$$

and hence

$$2t_3c = 2\,\frac{p}{\sigma}\left(a_1^2 \cos \alpha_1 \sin \alpha_1 + a_2^2 \cos \alpha_2 \sin \alpha_2\right)$$

$$= \frac{p}{\sigma}\left(a_1^2 \sin 2\alpha_1 + a_2^2 \sin 2\alpha_2\right)$$

Summing up the three parts, the total metallic cross section is found to be:

$$A_m = 2\,\frac{p}{\sigma}\left[a_1^2\left(\pi - \alpha_1 + \frac{1}{2}\sin 2\alpha_1\right) + a_2^2\left(\pi - \alpha_2 + \frac{1}{2}\sin 2\alpha_2\right)\right]$$

On the other hand, the area of the hollow cross section A_h describes the useful space in the fuselage. It is

$$A_h = a_1^2\left(\pi - \alpha_1 + \frac{1}{2}\sin 2\alpha_1\right) + a_2^2\left(\pi - \alpha_2 + \frac{1}{2}\sin 2\alpha_2\right)$$

It is seen that the ratio of the two areas

$$A_m/A_h = 2\,\frac{p}{\sigma}$$

does not depend upon the particular choice of the dimensions of the cross section. For a simple circular cylinder of radius a there is obtained by similar reasoning:

$$t = \frac{p}{\sigma} a$$

$$A_m = 2\pi at$$

$$= 2\pi \frac{p}{\sigma} a^2$$

$$A_h = \pi a^2$$

and hence

$$A_m/A_h = 2 \frac{p}{\sigma}$$

as before. This indicates that for the same inside space the same structural weight is required and one is freed from weight considerations when choosing that combination of a_1, a_2, α_1, and α_2 which seems best for other reasons The validity of this result is restricted to cross sections where the tie acts in tension, and this is exactly the configuration which is most interesting in aircraft construction. In practical applications, of course, additional stresses will change the picture to some extent, and the weight of different shapes will not be equal, but the important fact remains that there is no first-order loss or gain in choosing one or another of the sections compared.

Interaction between Shell and Rings

Bending of a cylindrical shell.- If the rings are not spaced closely enough to be considered as part of an anisotropic shell, the problem illustrated by figure 7 must be treated. Cut the shell in the plane of the ring and at its connection with the ring. The pressure p applied to the shell will lead to a hoop strain ϵ_ϕ which may be found from Hooke's law (3) and formulas (6a) to (6b) and consequently will lead to a radial displacement

$$w_o = a\epsilon_\phi$$

$$= \frac{pa^2}{E}\left(\frac{1 - \nu^2}{t} - \frac{\nu(1 - 2\nu)}{2t_x}\right)$$

The ring receives no load and, therefore, has no deformation. In order to close the gap between the ring and the deformed shell, add shearing forces T per unit length of the edges. In the ring of cross section A_R these shearing forces produce the stress

$$\sigma_R = \frac{2Ta}{A_R}$$

and hence the radial displacement

$$w_R = \frac{2Ta^2}{EA_R} \tag{7}$$

(More exactly, aa_1 should be written instead of a^2, where a_1 is the radius of the center line of the ring.)

For the shell, the force T is a transverse shear Q_x which produces bending stresses. In order to find them, some details of the theory of bending of an anisotropic cylinder must be developed. It is necessary to consider only the internal forces and moments shown on the shell element in figure 8: The hoop force N_ϕ, the bending moment M_x, and the transverse shear Q_x. They are all functions of x (fig. 7), as is the radial deflection w.

The forces and moments must satisfy the conditions of equilibrium of the shell element. They yield two equations:

$$\frac{dM_x}{dx} = Q_x \tag{8a}$$

$$a\frac{dQ_x}{dx} + N_\phi = 0 \tag{8b}$$

which, after elimination of Q_x, give the relation:

$$a\frac{d^2M_x}{dx^2} + N_\phi = 0 \tag{9}$$

The hoop force N_ϕ produces a hoop strain ϵ_ϕ which may be obtained from equations (3a) and (5a) to (5c) with $N_x = 0$. This strain leads to a radial displacement

$$w = a\epsilon_\phi$$

$$= N_\phi a \frac{t_x - \nu^2(t_x - t)}{Ett_x}$$

$$= \frac{N_\phi a}{D_\phi}$$

The constant $D_\phi = Et \dfrac{t_x}{t_x - \nu^2(t_x - t)}$, which has the dimension of a force per unit length, is the extensional rigidity of the shell in the direction of the hoop forces. Figure 9 shows that, in the range of practical interest, D_ϕ is only slightly greater than Et, and it is safe to say

$$N_\phi = Et \frac{w}{a} \tag{10}$$

The bending moment M_x produces a curvature d^2w/dx^2 of the generators. If I is the moment of inertia of the cross section of a stringer and the attached skin of width $a\delta$ divided by the distance $a\delta$ of the stringers,

$$M_x = EI \frac{d^2w}{dx^2} \tag{11}$$

Here too the coefficient EI is slightly influenced by the fact that the skin has a two-dimensional stress system. This refinement of the theory will not be discussed here. There is another circumstance, perhaps even more serious, which will also be neglected here: The centroid of the section to which I is referred is not exactly at the distance a from the axis of the cylinder but at a somewhat shorter distance. This influence may be studied with a more general set of equations, but since the difference of the two radii is not great, it will probably not be of first-order importance: however, it may be responsible for some second-order effects which otherwise might not be explained.

By introducing the expressions for N_ϕ and M_x into equation (9), the differential equation of the problem is obtained:

$$EI \frac{d^4w}{dx^4} + Et \frac{w}{a^2} = 0 \tag{12}$$

The general solution of this equation consists of four terms. Only those which are symmetrical with respect to the plane $x = 0$ are needed. They are:

$$w = C_1 \cosh \frac{\kappa x}{a} \cos \frac{\kappa x}{a} + C_2 \sinh \frac{\kappa x}{a} \sin \frac{\kappa x}{a}$$

with

$$\kappa = \sqrt[4]{\frac{ta^2}{4I}}$$

The boundary conditions at $x = l/2$ are that the slope dw/dx must be zero and that the deflection must assume a certain value w_1. (This will be discussed later.)

$$\left(\frac{dw}{dx}\right)_{x=l/2} = 0$$

$$w_{x=l/2} = w_1$$

Introducing the solution here, C_1 and C_2 are found and then

$$w = \frac{w_1}{\cosh \beta \sinh \beta + \cos \beta \sin \beta} \left[(\cosh \beta \sin \beta + \sinh \beta \cos \beta) \cosh \frac{2\beta x}{l} \cos \frac{2\beta x}{l} + (\cosh \beta \sin \beta - \sinh \beta \cos \beta) \sinh \frac{2\beta x}{l} \sin \frac{2\beta x}{l} \right]$$

with

$$\beta = \frac{\kappa l}{2a}$$

$$= \frac{l}{2\sqrt{2a}} \sqrt[4]{\frac{t}{I}}$$

The internal forces can now be found easily. From equations (8a) and (11) it follows that

$$Q_x = \frac{dM_x}{dx}$$

$$= EI \frac{d^3w}{dx^3}$$

$$= -\frac{Et\ell w_1}{2a^2\beta(\cosh \beta \sinh \beta + \cos \beta \sin \beta)}\left(\cosh \beta \sin \beta \cosh \frac{2\beta x}{\ell} \sin \frac{2\beta x}{\ell} + \right.$$

$$\left. \sinh \beta \cos \beta \sinh \frac{2\beta x}{\ell} \cos \frac{2\beta x}{\ell}\right)$$

For $x = \ell/2$ this is the force T applied to the edge of the shell:

$$T = -\frac{Et\ell w_1}{2a^2\beta} \frac{\cosh^2\beta - \cos^2\beta}{\cosh \beta \sinh \beta + \cos \beta \sin \beta} \tag{13}$$

Combining this with the preceding formula

$$Q_x = T \frac{\cosh \beta \sin \beta \cosh \frac{2\beta x}{\ell} \sin \frac{2\beta x}{\ell} + \sinh \beta \cos \beta \sinh \frac{2\beta x}{\ell} \cos \frac{2\beta x}{\ell}}{\cosh^2\beta - \cos^2\beta}$$

Introducing the solution w into equations (11) and (10) and expressing w_1 by T,

$$M_x = EI \frac{d^2w}{dx^2}$$

$$= -T \frac{\ell}{4\beta} \frac{1}{\cosh^2\beta - \cos^2\beta}\left[(\cosh \beta \sin \beta - \right.$$

$$\sinh \beta \cos \beta) \cosh \frac{2\beta x}{\ell} \cos \frac{2\beta x}{\ell} -$$

$$\left.(\cosh \beta \sin \beta + \sinh \beta \cos \beta) \sinh \frac{2\beta x}{\ell} \sin \frac{2\beta x}{\ell}\right]$$

and, adding the hoop force due to the pressure p,

$$N_\phi = pa + \frac{Etw}{a}$$

$$= pa - T\,\frac{2a\beta}{l}\,\frac{1}{\cosh^2\beta - \cos^2\beta}\left[(\cosh\beta \sin\beta + \sinh\beta \cos\beta)\cosh\frac{2\beta x}{l}\cos\frac{2\beta x}{l} + (\cosh\beta \sin\beta - \sinh\beta \cos\beta)\sinh\frac{2\beta x}{l}\sin\frac{2\beta x}{l}\right]$$

The magnitude of the shearing force T still has to be found. Write, for abbreviation, $T = -kw_1$, where k is defined by equation (13). Then the following deformations are found: Under the action of the internal pressure alone the shell has the deflection w_o given at the beginning of this section, and the ring, none. The additional load T bends the edge of the shell back, producing $w_1 = -T/k$, and the ring has a positive displacement $w_R = 2Ta^2/EA_R$ as was seen earlier.

Now, under the combined action of pressure p and shear T, the radial displacement of shell and ring must be the same

$$w_o - \frac{T}{k} = w_R$$

$$= \frac{2Ta^2}{EA_R}$$

From this equation

$$T = \frac{w_o}{\frac{2a^2}{EA_R} + \frac{1}{k}}$$

Upon the introduction of w_o and k this yields

$$T = \frac{\frac{p}{2}\left(\frac{1 - \nu^2}{t} - \frac{\nu(1 - 2\nu)}{2t_x}\right)}{\frac{1}{A_R} + \frac{\beta}{lt}\left(\frac{\cosh \beta \sinh \beta + \cos \beta \sin \beta}{\cosh^2\beta - \cos^2\beta}\right)} \tag{14}$$

With the numerical value of T from this formula, one may obtain from the preceding formulas values for N_ϕ and M_x. The complete solution of the mechanical problem of the interaction of the shell and the rings is now obtained.

The shear depends on many parameters, and no attempt has been made here to represent formula (14) by diagrams. However, the distribution of N_ϕ and M_x along a generator of the cylinder depends essentially on β. When β is small (closely spaced rings, heavy stringers), the picture looks somewhat like figure 10(a), and the case where it is adequate to represent the influence of the stringers by the effective thickness t_ϕ as defined by equation (2) is approached. But when β is great (rings far apart, light stringers), the internal forces are like those sketched in figure 10(b): In this case the influence of each ring is locally restrained.

Floating skin.- From figure 10 it appears that there is not much virtue in providing rings to help the skin carry the cabin pressure because the skin alone can do that well enough and the rings only cause trouble. The rings disturb the simple stress system considerably, and the force $2T$ transmitted from the shell to the ring produces a highly undesirable tensile stress in the rivets which connect the skin to the ring.

However, the rings are needed for many important purposes. They help to introduce the local load gently into the shell, they support the stringers against buckling, and they stiffen the shell as a whole to prevent a collapse by large-scale buckling. The problem is, how does one make the rings available for all these purposes without introducing the forces T?

The solution is the floating skin. Its basic idea may be explained from equation (14). If the rings are very weak, $A_R \longrightarrow 0$, the denominator of this formula becomes infinite, and $T = 0$. The term $2/A_R$ comes from w_R, equation (7), and represents the deformability of the ring by a radial load T, or, more exactly, the radial displacement of

those points where the ring is fixed to the shell (skin and stringers). This deformability may be increased easily without weakening the ring. It is only necessary to intersperse an elastic element between the ring proper and the shell (including stringers) as it is indicated by the sketch, figure 11. Formula (7) must then be replaced by

$$w_R = \frac{2Ta^2}{EA_R} + w_R'$$

$$= \frac{2Ta^2}{EA_R} + cT$$

c being an elastic constant depending on the shape and size of the connecting link between ring and skin. In formula (14) it is then necessary to write

$$\frac{2}{A_R} + \frac{Ec}{a^2}$$

instead of $2/A_R$ and now there is the possibility of making the denominator as great as desired. Of course, such a flexible connection is only worth while if the denominator in equation (14) is appreciably increased by adding the term Ec/a^2.

Doors and Windows

When the cabin is under pressure, the door must, of course, be closed, but it cannot be expected that the door panel will be very efficient in transmitting hoop forces N_ϕ or longitudinal forces N_x across the door opening. Both have to be carried around it by the door frame, and this disturbance of the smooth flow of forces will certainly lead to an increase in structural weight. In order to keep this increase as small as possible, some details of the local stress system will have to be studied.

Since the door needs a frame, it is reasonable to extend the lateral parts of this frame all around the shell as two of its rings. Outside of the part of the fuselage limited by these rings the hoop force does not meet with any obstruction. The problem is, what must be done with the forces which are intercepted by the sill and the head of the frame? With the usual dimensions of fuselages and doors these forces are considerable. A door frame strong enough to resist them would be a heavy structure,

but worse than that, it would not accept the load. It would deflect in the direction of the pull, and the deflection would lead to a decrease of the pull.

It seems wise, therefore, to allow the shell itself to do that which it can do so easily and to give the horizontal members of the door frame only that stiffness which is required to press the door firmly against it, that is, bending stiffness against radial forces. It is necessary, then, to solve the following mechanical problem (fig. 12): A cylindrical shell extending over an angle $\alpha < 360^\circ$ is limited by two circular rings and by two straight end members. These end members have no rigidity against bending in the tangential plane to the cylinder, but they have enough cross section to be considered as inextensible for our purposes. The shell is subjected to an internal pressure p.

The stress system set up under these conditions may be split into two parts: One is a hoop force $N_\phi = pa$, acting everywhere (also on the straight edge) and resisting to the load p; the other one is a system of internal forces produced by an external load $N_\phi = -pa$ applied to the edge members and canceling there the force pa of the elementary solution.

The task which is now to be done is to find this second stress system. In the theory of shells it is shown that the tangential load $-pa$ cannot be carried by the shell without resorting to bending stresses. There are different methods of treating this bending problem; this is a simple one. Although its application in this case may not be entirely legitimate, it will give a fair idea of what is happening, and that should be enough.

The problem may be reduced to a differential equation for the bending moment M_ϕ (for the notations, see figs. 8 and 12; for more details see reference 2, p. 139, or reference 3):

$$M_\phi'''' + (2 + \nu)M_\phi''''' + 2M_\phi''' + (1 + 2\nu)M_\phi'''' + 2(2 + \nu)M_\phi''' + M_\phi'' + \nu M_\phi'''''' + (1 + \nu)^2 M_\phi'''' + (2 + \nu)M_\phi'' + \frac{1 - \nu^2}{k} M_\phi'''' = 0 \quad (15)$$

Here dots indicate derivatives with respect to ϕ, primes indicate derivatives with respect to the dimensionless coordinate x/a, and k is the shell parameter

$$k = \frac{t^2}{12a^2}$$

It may easily be verified that

$$M_\phi = Ce^{m\phi} \sin \frac{\lambda x}{a}$$

is a solution of the differential equation. Here λ is still an arbitrary constant. Write

$$\lambda = \frac{n\pi a}{l}$$

where n is a positive integer; the discussion will later be confined to $n = 1$.

When the solution is introduced into the differential equation, it is found that m must satisfy a certain algebraic equation. After some drastic simplifications (reference 4) it may be brought into the following form:

$$(m^2 + 1)^2 m^4 + \frac{1 - \nu^2}{k} \lambda^4 = 0$$

This equation has the complex solutions

$$m = \pm\sqrt{-\frac{1}{2} \pm \sqrt{\frac{1}{4} \pm i\lambda^2\sqrt{\frac{1 - \nu^2}{k}}}} \approx \pm\sqrt{\pm\sqrt{\pm in^2\zeta}} \qquad (16)$$

with

$$\zeta = \sqrt{\frac{\pi a}{l}\sqrt{\frac{2a}{t}\sqrt{3(1 - \nu^2)}}}$$

When any one of the eight complex values m is introduced into the formula for M_ϕ, one elementary solution is obtained. They all show a variability in x-direction according to $\sin n\pi x/l$. The same factor will appear in the corresponding hoop forces N_ϕ. When it is desired to use these solutions to describe the stresses due to a uniform distribution

$$N_\phi = -pa$$

of the hoop force on the edge $\phi = 0$, this distribution has to be resolved into its harmonic components:

$$-pa = -\frac{4pa}{\pi}\left(\sin\frac{\pi x}{l} + \frac{1}{3}\sin\frac{3\pi x}{l} + \frac{1}{5}\sin\frac{5\pi x}{l} + \ldots\right)$$

The discussion will be confined here to the first term of this series which will show the essential features of the stress pattern. Correspondingly, set $n = 1$.

The set of eight elementary solutions which is obtained from the eight possible values of m may be replaced by an equivalent set of eight linear combinations, each of which is a product of an exponential and a trigonometric function of $\kappa_1\phi$ or $\kappa_2\phi$, where

$$\kappa_1 = \zeta\sqrt{n}\cos 22.5^\circ$$

$$\kappa_2 = \zeta\sqrt{n}\sin 22.5^\circ$$

Using a suitable set of boundary conditions to determine the constants C with which these solutions must be multiplied, solutions for many cases of loading and supporting the edge may be found. The full expression for the bending moment M_φ and the values of the displacements u (in x-direction) and w (radially outward) for the edge $\varphi = 0$ are given here for three important cases:

(1) Normal forces $N_\phi = F_1 \sin\frac{\pi x}{l}$, applied to a free (unsupported) edge,

$$M_\phi = -\frac{F_1 a}{\zeta^2}\left(\sqrt{2} + 1\right)\left[e^{-\kappa_1\phi}\left(\cos\kappa_2\phi + \sqrt{2}\sin\kappa_2\phi\right) - e^{-\kappa_2\phi}\cos\kappa_1\phi\right]\sin\frac{\pi x}{l} \tag{17a}$$

with the displacements at the edge $\phi = 0$,

$$u = -\frac{F_1 a}{Et\lambda^3}\left[\left(\sqrt{2} + 1\right)\sqrt{2}\zeta^2 - 1 - \nu\lambda^2\right]\cos\frac{\pi x}{l}$$

$$w = -\frac{F_1 a}{Et\lambda^4}\left[\left(\sqrt{2}+1\right)^2\zeta^4 + \left(1-2\lambda^2\right)\left(\sqrt{2}+1\right)\sqrt{2}\zeta^2 + \left(2+\nu-\lambda^2\right)\lambda^2\right] \sin\frac{\pi x}{l}$$

(2) Shearing forces $N_{\phi x} = F_2 \cos\frac{\pi x}{l}$, applied to a free edge,

$$M_\phi = -\frac{F_2 a\lambda}{2\zeta^3}\sqrt{2+\sqrt{2}}\left\{e^{-\kappa_1\phi}\left[\cos\kappa_2\phi + \left(\sqrt{2}+1\right)\sin\kappa_2\phi\right] - e^{-\kappa_2\phi}\left[\cos\kappa_1\phi + \left(\sqrt{2}-1\right)\sin\kappa_1\phi\right]\right\}\sin\frac{\pi x}{l} \tag{17b}$$

with the displacements at the edge $\phi = 0$,

$$u = -\frac{F_2 a\zeta}{Et\lambda^2}\sqrt{2}\sqrt{2+\sqrt{2}}\cos\frac{\pi x}{l}$$

$$w = -\frac{F_2 a\zeta}{Et\lambda^3}\sqrt{2}\sqrt{2+\sqrt{2}}\left(\zeta^2+1-2\lambda^2\right)\sin\frac{\pi x}{l}$$

(3) Combined action of a shearing force $N_{\phi x} = F_3 \cos\frac{\pi x}{l}$ and a transverse force $Q_\phi = -\lambda F_3 \sin\frac{\pi x}{l}$, applied to a free edge

$$M_\phi = -\frac{F_3 a\lambda}{2\zeta}\sqrt{2+\sqrt{2}}\left\{e^{-\kappa_1\phi}\left[\left(\sqrt{2}+1\right)\cos\kappa_2\phi + \left(2\sqrt{2}+1\right)\sin\kappa_2\phi\right] - e^{-\kappa_2\phi}\left[\left(\sqrt{2}+1\right)\cos\kappa_1\phi - \sin\kappa_1\phi\right]\right\}\sin\frac{\pi x}{l} \tag{17c}$$

with the displacements at the edge $\phi = 0$,

$$u = -\frac{F_3 a\zeta^3}{Et\lambda^2}\sqrt{2}\sqrt{2+\sqrt{2}}\cos\frac{\pi x}{l}$$

$$w = -\frac{F_3 a\zeta^3}{Et\lambda^3}\sqrt{2}\sqrt{2+\sqrt{2}}\left[\left(\sqrt{2}+1\right)\zeta^2 + 1 - 2\lambda^2\right]\sin\frac{\pi x}{l}$$

Coming back to the original problem represented by figure 12, the bending moment M_ϕ may be found by superposing the three solutions (equations (17a) to (17c)) with appropriate values of the constants F_1, F_2, and F_3. These can be found from three boundary conditions at the edge $\phi = 0$.

The first harmonic of the load pa shown in figure 12 is $N_\phi = -\frac{4pa}{\pi} \sin \frac{\pi x}{l}$. In order to give N_ϕ this value, it is necessary to set

$$F_1 = -\frac{4pa}{\pi}$$

and this is the first of three conditions. The other two follow from the deformation which the door frame imposes on the shell. Since the cross section of this frame is assumed to be large enough to neglect axial deformations, $u = 0$ at $\phi = 0$ for the shell. Another assumption formulated previously is that the door frame will not deflect very much in the w-direction. Therefore, $w = 0$ at $\phi = 0$ for the shell.

When u and w are expressed as sums of the contributions of F_1, F_2, and F_3, according to the formulas given before, and set equal to zero, there are two linear equations from which F_2 and F_3 may be found. The result is as follows:

$$F_2 = \frac{pa}{\pi\zeta^3\lambda} \sqrt{2}\sqrt{2 - \sqrt{2}} \left[\left(\sqrt{2} + 1\right)\zeta^4 - \left(\sqrt{2} + 1\right)\left(1 + \nu\lambda^2\right)\zeta^2 - 1 - 2\nu\lambda^2 + (1 + 2\nu)\lambda^4\right]$$

$$F_3 = \frac{pa}{\pi\zeta^5\lambda} \sqrt{2}\sqrt{2 - \sqrt{2}} \left[\left(\sqrt{2} + 1\right)\zeta^4 - \left(1 - \nu\lambda^2\right)\zeta^2 + 1 + 2\nu\lambda^2 - (1 + 2\nu)\lambda^4\right]$$

The bending moment M_ϕ due to the combined action of F_1, F_2, and F_3 can now be computed; going back through details of the theory

which have not been reproduced here, the hoop force N_ϕ and the longitudinal force N_x in the shell can also be found.

This has been done for an illustrative example, where

$$\lambda = 6$$

$$\frac{1 - \nu^2}{k} = 14 \times 10^6$$

$$\nu = 0.3$$

The results are plotted in figure 13 over the circumference of a cross section through the fuselage.

This diagram shows the following features which are of practical interest:

(1) The disturbance produced by the door opening is restricted to a rather small part of the shell. At an angular distance of 30° from the edge it has practically vanished.

(2) The disturbance in the hoop force is without importance. It is only slightly higher locally than in the undisturbed part of the shell.

(3) There are considerable stresses in the x-direction. The forces N_x shown in the diagram are, of course, additional to forces which may exist from other causes. In particular, there is a zone of tensile stress near the edge. When taken together with a compressive force in the adjacent bar of the door frame, these stresses are comparable with bending stresses in a beam of span l, which receives the load $N_\phi = pa$ from the undisturbed shell and is supported on the two rings shown in figure 12.

(4) The forces N_x are arranged in alternating tension and compression zones of approximately equal width and decreasing intensity. The width is such that in usual fuselages it may be of the same order as the distance between stringers. If stringers were placed at the zeros of N_x, they would not influence our problem. This justifies the procedure used, which is based on the assumption of an isotropic shell without stiffeners.

(5) If an additional stringer were provided right at the peak of N_x, the stress distribution would, of course, be changed considerably. The

essential effect of this measure would be beneficial: The stringer would share the axial load with the shell. Therefore, it may be suggested that only the width of the first tension zone be determined, and a good stringer be provided at its center, that is, at a distance of $90°/\kappa_1$ from the door frame.

Bulkheads

General formulas for shells of revolution.- A cylindrical pressure cabin must be closed at its end by a bulkhead. This bulkhead may be constructed as a flat wall built up of vertical and horizontal beams and a metal sheet. The beams have to transmit the air pressure by bending stresses to the circumference of the bulkhead, from where it can be transferred to the cylindrical cabin wall. Since the total air pressure on the bulkhead is a force of considerable magnitude, a flat bulkhead will result in a heavy construction, which should be avoided if possible.

The preferable shape of a bulkhead is that of a shell similar to a boiler end. When the cabin has a circular cross section, such a bulkhead will be a shell of revolution. As a basis for its stress analysis a short account of the theory of such shells will be given here.

Figure 14 shows the middle surface of a shell of revolution; its intersections with planes normal to its axis are parallel circles, and its intersections with planes containing the axis are all equal to each other and are called meridians. At all points of a parallel circle the angle ϕ between its plane and a tangent to the meridian has the same value and is therefore characteristic for this circle. The angle between the plane of a meridian and the vertical will be called θ. Since a point of the shell is determined by the parallel and the meridian on which it lies, the angles ϕ and θ may be used as coordinates on the shell.

If the shell is cut along a parallel circle (fig. 15), the stresses transmitted there can be found. As is usual in shell theory, equations are not written for the stress but for the meridional force N_ϕ which acts on the unit length of the circle. This force has the direction of the meridian. The resultant of all the meridional forces acting on one parallel circle is horizontal and of the magnitude $N_\phi(\sin \phi)2\pi r$, and it must be equal to the resultant $R = \pi r^2 p$ of the air pressure. Hence

$$N_\phi = \frac{R}{2\pi r \sin \phi}$$

$$= \frac{pr}{2 \sin \phi} \qquad (18a)$$

When the shell is cut along a meridian, internal forces, that is, the hoop forces N_θ, are found, but they are not the same at all points of the meridian and, therefore, cannot be found as simply as N_ϕ. A shell element limited by two adjacent meridians and two adjacent parallel circles (fig. 16) has to be cut out. The sides of this element, which are parts of meridians, have the length $r_1\,d\phi$, where r_1 is the radius of curvature of the meridian. The other two sides have the length $r\,d\theta$ (slightly different from each other because r is not the same on both parallel circles). The equilibrium of the forces $N_\phi(r\,d\theta)$, $N_\theta(r_1\,d\phi)$, and the air pressure $p(r\,d\theta)(r_1\,d\phi)$ in the direction of a normal to the shell yields the equation

$$N_\phi(r\,d\theta)d\phi + N_\theta(r_1\,d\phi)d\theta \sin\phi = p(r\,d\theta)(r_1\,d\phi)$$

The factor $\sin\phi$ in the second term comes from the fact that the resultant of the hoop forces lies in the plane of the parallel circle and has to be projected on the normal to the shell. The equation may be simplified to

$$\frac{N_\phi}{r_1} + \frac{N_\theta}{r}\sin\phi = p$$

Introducing N_ϕ from equation (18a) into this equation,

$$N_\theta = \frac{pr}{\sin\phi}\left(1 - \frac{r}{2r_1\sin\phi}\right) \tag{18b}$$

Equations (18a) and (18b) are sufficient to find the internal forces N_ϕ and N_θ when the shape of the shell is known. In order to permit the best use of the space in the pressure cabin and in the fuselage at its rear, an ideal bulkhead should be as flat as possible. This might lead to a bulkhead designed to meet the cylindrical cabin wall at an angle, as shown in figure 17(a). At the edge of the bulkhead equation (18a) will yield a certain value of the force N_ϕ which, of course, must have the direction of a tangent to the meridian. Now this force cannot be transmitted to the cylinder because this shell can only resist a force N_x having the direction of a generator. The difference, that is, the radial component of N_ϕ, must be transmitted to a stiffening ring. It leads

there to a compressive force of considerable magnitude. The corresponding deformation, a decrease of the ring diameter, fits in no way to that of the cylinder and no better to that of the bulkhead. Therefore, all the trouble with bending stresses described in the section entitled "Bending of a Cylindrical Shell" arises here again but in a much more serious magnitude. The meridian of the bulkhead should, therefore, always end with a tangent parallel to the generators of the cylindrical cabin wall.

At the center of the bulkhead $r = 0$ and $\phi = 0$, and formulas 18(a) and 18(b) become indefinite. If the meridian has a finite radius of curvature r_1 at this point, then, in its vicinity the relation

$$r = r_1 \sin \phi$$

holds. Introducing it into equations (18), they yield

$$N_\phi = N_\theta = \frac{pr_1}{2} \tag{18c}$$

The tendency to make the bulkhead as flat as possible might lead to a meridian with an extremely feeble curvature in the central part. In the extreme case, for the curvature $1/r_1 = 0$, the stresses become infinite. This is illustrated by figure 18. The meridian in the upper half is a biquadratic parabola $a^3x = r^4$, and the diagrams of the forces N_ϕ and N_θ show the consequences of insufficient curvature of the shell. The lower half of the figure shows how easily the situation can be improved. Here the central part of the shell is replaced by a spherical segment, and at once the stresses are reduced to a moderate magnitude.

It may be mentioned that the meridian chosen for this example does not fulfill the condition of a smooth transition to a cylinder, and, therefore, cannot be recommended even in the improved form, but the essential effect shown in figure 18 is, of course, true for any other shape with insufficient curvature.

Ellipsoidal bulkhead.- An oblate ellipsoid (fig. 19) used as a bulkhead provides a good compromise between the desire to avoid dead angles and dark corners and the necessity of providing a smooth flow of forces. Relations between the radii r, r_1, and ϕ may be found from the equation of the elliptic meridian. They are:

$$r = \frac{a^2 \sin \phi}{\left(a^2 \sin^2\phi + b^2 \cos^2\phi\right)^{1/2}}$$

$$r_1 = \frac{a^2 b^2}{\left(a^2 \sin^2\phi + b^2 \cos^2\phi\right)^{3/2}}$$

When these are introduced into equations (18a) and (18b),

$$N_\phi = \frac{pa^2}{2\left(a^2 \sin^2\phi + b^2 \cos^2\phi\right)^{1/2}}$$

$$N_\theta = \frac{pa^2}{2b^2} \frac{b^2 - \left(a^2 - b^2\right) \sin^2\phi}{\left(a^2 \sin^2\phi + b^2 \cos^2\phi\right)^{1/2}}$$

These formulas describe completely the stresses in the bulkhead. They are not limited to a shell of constant thickness, hence the local stresses may be found simply by dividing by the local thickness t of the shell:

$$\sigma_\phi = N_\phi/t$$

$$\sigma_\theta = N_\theta/t$$

The stresses at two points are of main interest: The center $\phi = 0^\circ$ and the edge $\phi = 90^\circ$. In the center is found a biaxial tension

$$\sigma_\phi = \sigma_\theta$$

$$= \frac{pa^2}{2bt}$$

which determines the wall thickness. At the edge, the force N_ϕ transmitted to the cylindrical fuselage is independent of b and is the same for all ellipsoids (and for any other shape of bulkhead with smooth

transition to the cylinder). The hoop force N_θ depends largely on the ratio a/b of the axes. If $b = 0.707a$ it becomes zero, and if the ellipsoid is still flatter the hoop force will be a compression. Since it is desirable to build the bulkhead as flat as possible, this fact deserves special attention. The compressive stress may be rather high, but it is confined to a small zone. Figures 20(a) and 20(b) show two examples of the stress distribution. In any case it will be wise to provide for a stiffening ring at the connection between the bulkhead and the fuselage.

The compressive hoop stress has still another consequence which needs consideration. It produces an elastic deformation, which decreases the diameter of the boundary circle of the bulkhead. On the other hand, the diameter of the cylindrical wall of the fuselage will increase in the part in front of the bulkhead as a consequence of the positive hoop stress in a cylindrical shell, and will not change at all in the part behind the bulkhead where there is no internal pressure. The deformations of the three shells look somewhat as shown in figure 21. Since the shells are connected to each other, such a discrepancy cannot exist in reality but will be prevented by a system of bending stresses in the boundary zones of all three parts. In boilers and other pressure vessels these bending stresses are rather serious and means to avoid them are desirable. In pressure cabins they may be of some minor importance, but it is certainly better to eliminate them as far as possible.

The discrepancy between the two cylindrical parts is, of course, unavoidable, but the edge deformation of the bulkhead should lie between those of the two cylinders. That means, at least, that the hoop force N_ϕ must be positive. A hemisphere would fulfill this condition perfectly, but as a bulkhead it would lead to poor utilization of space. A better solution is to turn the ellipsoidal bulkhead with its convex side toward the pressure cabin (fig. 22(a)). Then the previous formulas are still applicable, but the signs of all stresses are reversed. That is desirable at the edge but certainly not in the center, where compressive stresses create a buckling problem. This will be avoided by the bulkhead shown in figure 22(b). The trouble with this shape is that the membrane stresses at the sharp edge between the convex and concave shells cannot make equilibrium with each other without the help of a stiffening ring. This is shown by figure 23. The two meridional forces N_ϕ shown there, one a tension and the other a compression, will have the same horizontal component and thus assure the axial equilibrium of the shell; but their radial components are both directed outward and, therefore, cannot equilibrate each other. If a ring is provided, they may both be transmitted to it as shown, leading to a compressible hoop force in the ring. But here a new difficulty arises. The hoop strains of the three parts will not fit together and will again lead to bending

stresses. It may be that they will turn out to be less serious in a particular case, but at least they are now at a place where they do not produce quilting of the surface of the fuselage.

Bulkheads with improved boundary effects.- A more promising method to avoid excessive bending stresses would be to choose another shape of the meridian. The fact that a hemisphere gives just what is wanted, an edge deformation halfway between zero and that of the cylindrical cabin wall, indicates that the meridian must begin with a curvature $1/a$ at the edge. In order to make the bulkhead flat, the curvature should then increase and later become very small when the center is approached. This is schematically shown in figure 24, but the idea cannot be executed in this form because any discontinuity in the curvature again will produce those local bending stresses that are to be eliminated.

What is needed is a curve having the same general shape but a smooth transition of curvature. Such a curve may be found in several ways.

One is a modification of the Cassinian curves (see also reference 5). Using the coordinates x and r in a meridional plane as shown in figure 24, the equation

$$\left(n^2x^2 + r^2\right)^2 - 2A^2\left(n^2x^2 - r^2\right) = B^4 \tag{19}$$

describes a Cassinian curve, if $n = 1$. With $n > 1$ the curves are flattened and for $2 < n < 3$ assume a reasonable shape. The parameters A and B must be chosen so that for $x = 0$ the ordinate becomes $r = a$ and the radius of curvature is $r_1 = a$. This yields

$$A = a\sqrt{\frac{n^2 - 1}{n^2 + 1}}$$

$$B = a\sqrt[4]{\frac{3n^2 - 1}{n^2 + 1}}$$

The radius of curvature at the center of the bulkhead will then be

$$r_1 = a\,\frac{n^3}{2n^2 - 1}\sqrt{\frac{3n^2 - 1}{n^2 + 1}}$$

With these data the internal forces at the most interesting points can be found. At the edge equations (18a) and (18b) with $r = r_1 = a$ and $\phi = 90^\circ$ give:

$$N_\phi = \frac{pa}{2}$$

$$N_\theta = \frac{pa}{2}$$

At the center equation (18c) must be used and

$$N_\phi = N_\theta$$

$$= \frac{pa}{2} \frac{n^3}{2n^2 - 1} \sqrt{\frac{3n^2 - 1}{n^2 + 1}}$$

is obtained.

But this is not enough. To be safe from surprises, one must have the stress distribution along the meridian. It can be found by the following procedure.

Assume x and from equation (19) find r, or vice versa, depending on which will give the greater accuracy. Then compute

$$r' = \frac{dr}{dx}$$

$$= -\frac{n^2 x}{r} \frac{n^2 x^2 + r^2 - A^2}{n^2 x^2 + r^2 + A^2}$$

$$\frac{r}{\sin \phi} = r\sqrt{1 + (r')^2}$$

$$r'' = \frac{d^2 r}{dx^2}$$

$$= \frac{r'}{x} - \frac{(r')^2}{r} - \frac{n^2 x}{r} \frac{4A^2(n^2 x + rr')}{(n^2 x^2 + r^2 + A^2)^2}$$

$$\frac{r}{r_1 \sin \phi} = \frac{rr''}{1 + (r')^2}$$

Now formulas (18a) and (18b) may be applied.

This was done for $n = 2$ and the results shown in figure 25 were obtained. The hoop force N_θ falls to zero and rises at the center of the bulkhead toward the value previously mentioned. If $n > 2$ is chosen, the hoop force will become negative, and very much so if n is too great. This, of course, should be avoided.

Bulkhead for double cylinders.- In a double-cylinder cabin the two cylinders may have their bulkheads at different stations. Between the two bulkheads the longer cylinder must have a full circular cross section, and its intersection with the first bulkhead leads to a difficult stress problem.

This situation is eased considerably if it is possible to have both bulkheads at the same cross section. Their shapes may then be chosen such that they intersect in a plane horizontal curve. This will be the case when they are oblate ellipsoids with the ratio $b:a = b':a'$. They may then be derived by affine transformation from two spheres as indicated by figure 26.

A reinforcing ring must be provided along the intersection of the two shells. It will now be shown that this ring, which has the shape of a half-ellipse, will be stressed in its own plane only, and, with a certain exception, will even be free from bending stresses.

In the case of two spheres this is evident. Introduce coordinates ϕ, ϕ', and θ as shown in figure 26. If the two shells are inflated by a pressure p, the internal forces will be

$$N_\phi = N_\theta = \frac{1}{2} pa$$

in the upper shell and

$$N_\phi' = N_\theta' = \frac{1}{2} pa'$$

in the lower. The forces N_ϕ for $\phi = 180^\circ - \alpha$ and N_ϕ' for $\phi' = 180^\circ - \alpha'$ act on the ring as shown in figure 27. Since

$$a \sin \alpha = a' \sin \alpha'$$

$$= c$$

the vertical components $N_\phi \sin \alpha$ and $N_\phi' \sin \alpha'$ balance each other and the horizontal components combine to a uniform radial load, producing a positive hoop force

$$F = c \frac{1}{2} p(a \cos \alpha + a' \cos \alpha')$$

in the ring.

When there are two ellipsoids, the stress analysis is not so simple. One might think of using the solution given under the section entitled "Ellipsoidal Bulkhead" for a single ellipsoid and of determining from it the forces acting on the elliptic ring. But there is no reason to believe that the axial symmetry assumed in deriving that solution still exists when part of the shell has been cut away and its symmetry thus destroyed. The clue to the solution is the idea that the ring shall be free of bending moments, and it has only to be shown that a solution with this property exists, that it is unique, and how to find it.

To fulfill this program, some notions of the theory of affine shells are needed (for details see references 2, 3, and 5). They will be presented here as applied to the particular problem to be solved.

In addition to the curvilinear coordinates ϕ,θ and ϕ',θ on the two spheres, two systems of rectangular coordinates are now introduced: x, y, and z for the ellipsoids and x^*, y^*, and z^* for the spheres. The simple geometrical relation between the two shells is represented by

$$x = nx^*$$

$$y = y^*$$

$$z = z^*$$

with $n = b/a$. As curvilinear coordinates on the ellipsoids the values of ϕ (or ϕ') and θ for the corresponding points on the spheres are used. These coordinates do not represent angles that can be measured on the ellipsoids, but each pair of values ϕ,θ defines

clearly one point on the shell, and this is all that coordinates are expected to do.

A shell element is cut out of the upper sphere by two meridians θ and $\theta + d\theta$ and by two parallels ϕ and $\phi + d\phi$. It has the area

$$dA^* = a^2 \sin \phi \, d\phi \, d\theta$$

When it is projected on the planes (y^*,z^*), (z^*,x^*), and (x^*,y^*), the projected areas are found:

$$dA_x{}^* = dA^* \sin \phi \cos \theta$$

$$dA_y{}^* = dA^* \sin \phi \sin \theta$$

$$dA_z{}^* = dA^* \cos \phi$$

The element of the bulkhead shell is simply the projection of the element dA^* on the ellipsoid. Both have the same projection on the yz-plane, but the other two projections are reduced in the ratio n:1:

$$\begin{aligned} dA_x &= dA_x{}^* \\ &= dA^* \sin \phi \cos \theta \end{aligned}$$

$$\begin{aligned} dA_y &= n \, dA_y{}^* \\ &= \frac{b}{a} dA^* \sin \phi \sin \theta \end{aligned}$$

$$\begin{aligned} dA_z &= n \, dA_z{}^* \\ &= \frac{b}{a} dA^* \cos \phi \end{aligned}$$

When the ellipsoid is inflated by an internal pressure p, the force acting on the element is $p \, dA$ and has the rectangular components $p \, dA_x$, $p \, dA_y$, and $p \, dA_z$ parallel to the axes x, y, and z. This load produces internal forces transmitted at the four sides of the shell

element dA. On each side of the element this force lies in a tangential plane to the shell and may be resolved into a normal and a shear component. Something better can be done: Oblique components parallel to the coordinate lines ϕ = Constant and θ = Constant can be used. These forces divided by the length ds_ϕ or ds_θ of the line element are called N_ϕ, N_θ, and $N_{\phi\theta}$, as indicated in figure 28.

A simple relation between these forces and a certain system of internal forces N_ϕ^*, N_θ^*, and $N_{\phi\theta}^*$ in the sphere will now be established. These forces must, of course, lie on tangents to the sphere, and they will be chosen in such a way that they have the same projections on the yz-plane as the corresponding forces in the ellipsoid. Then both will have the same components in the directions y and z, but the x-components of the forces N in the ellipsoid will equal n times the x-components of the forces N^* in the sphere.

The forces N^* of the sphere will be in equilibrium with a load which has the same y- and z-components as that applied to the ellipsoid, but $1/n$ times its x-component.

If the load components per unit area dA^* of the sphere are denoted by p_x^*, p_y^*, and p_z^*,

$$p_x^* \, dA^* = \frac{1}{n} p \, dA_x$$

$$= p \frac{a}{b} dA^* \sin \phi \cos \theta$$

$$p_y^* \, dA^* = p \, dA_y$$

$$= p \frac{b}{a} dA^* \sin \phi \sin \theta$$

$$p_z^* \, dA^* = p \, dA_z$$

$$= p \frac{b}{a} dA^* \cos \phi$$

and hence the loads per unit area of the surface of the sphere are

$$\left.\begin{aligned} p_x^* &= p\,\frac{a}{b}\sin\phi\cos\theta \\ p_y^* &= p\,\frac{b}{a}\sin\phi\sin\theta \\ p_z^* &= p\,\frac{b}{a}\cos\phi \end{aligned}\right\} \qquad (20)$$

If the forces set up in the spherical shell by this load can be found, it is only necessary to project them on the tangential plane of the ellipsoid and to refer to the unit length of the ellipsoid's line element and then the forces in the ellipsoidal bulkhead will be obtained.

To make the stress analysis for the sphere along conventional lines, the loads given by equation (20) are transformed into the components X^*, Y^*, and Z^* as shown in figure 28:

$$\begin{aligned} X^* &= -p_x^*\sin\theta + p_y^*\cos\theta \\ &= -\frac{p\left(a^2 - b^2\right)}{2ab}\sin\phi\sin 2\theta \end{aligned}$$

$$\begin{aligned} Y^* &= \left(p_x^*\cos\theta + p_y^*\sin\theta\right)\cos\phi - p_z^*\sin\phi \\ &= \frac{p\left(a^2 - b^2\right)}{2ab}\cos\phi\sin\phi(1 + \cos 2\theta) \end{aligned}$$

$$\begin{aligned} Z^* &= \left(p_x^*\cos\theta + p_y^*\sin\theta\right)\sin\phi + p_z^*\cos\phi \\ &= \frac{p}{2ab}\left[2b^2 + \left(a^2 - b^2\right)\sin^2\phi(1 + \cos 2\theta)\right] \end{aligned}$$

These expressions have the form

$$X^* = X_o^* + X_2^* \sin 2\theta$$

$$Y^* = Y_o^* + Y_2^* \cos 2\theta$$

$$Z^* = Z_o^* + Z_2^* \cos 2\theta$$

showing the harmonic constituents of orders 0 and 2.

The first term on the right is a load with rotational symmetry:

$$X_o^* = 0$$

$$Y_o^* = \frac{p(a^2 - b^2)}{2ab} \cos \phi \sin \phi$$

$$Z_o^* = \frac{p}{2ab}\left[2b^2 + (a^2 - b^2) \sin^2\phi\right]$$

Simple formulas, which will not be reproduced here, lead to the internal forces:

$$\left.\begin{aligned} N_\phi^* &= N_{\phi o}^* \\ &= \frac{pb}{2} \\ N_\theta^* &= N_{\theta o}^* \\ &= \frac{p}{2b}\left[b^2 + (a^2 - b^2)\sin^2\phi\right] \\ N_{\phi\theta}^* &= 0 \end{aligned}\right\} \qquad (21)$$

These formulas are valid for the upper sphere of radius a. For the lower sphere it is necessary to write simply a', b', and ϕ', instead of a, b, and ϕ, respectively.

The second harmonic of the load,

$$X_2^* = -\frac{p(a^2 - b^2)}{2ab} \sin \phi$$

$$Y_2^* = \frac{p(a^2 - b^2)}{2ab} \cos \phi \sin \phi$$

$$Z_2^* = \frac{p(a^2 - b^2)}{2ab} \sin^2 \phi$$

may not be handled so easily. It leads to forces which depend also on a sine or cosine of 2θ and may be written as

$$N_\phi^* = N_{\phi 2}^* \cos 2\theta$$

$$N_\theta^* = N_{\theta 2}^* \cos 2\theta$$

$$N_{\phi\theta}^* = N_{\phi\theta 2}^* \sin 2\theta$$

The basic formulas connecting $N_{\phi 2}^*$, $N_{\theta 2}^*$, and $N_{\phi\theta 2}^*$ with the load components X_2^*, Y_2^*, and Z_2^* may be found in the literature (reference 2, pp. 37 to 44, or reference 3). They lead to a solution having two free constants for each of the spheres. One constant in each pair may be determined from the condition that the stresses are finite at $\phi = 0$ and $\phi' = 0$. The other two are still to be determined. In this way are obtained

$$N_{\phi 2}^{*} = \frac{p\left(a^2 - b^2\right)}{2b} + \frac{C}{2(1 + \cos \phi)^2}$$

$$N_{\phi\theta 2}^{*} = - \frac{p\left(a^2 - b^2\right)}{2b} \cos \phi - \frac{C}{2(1 + \cos \phi)^2}$$

$$N_{\theta 2}^{*} = - \frac{p\left(a^2 - b^2\right)}{2b} \cos^2 \phi - \frac{C}{2(1 + \cos \phi)^2}$$

for the upper shell and corresponding formulas for the lower, containing another constant C'.

From these forces the ring receives a radial load $\left(N_{\phi 2}^{*} \cos \alpha + N_{\phi 2}^{*'} \cos \alpha'\right) \cos 2\theta$, a vertical load $\left(N_{\phi 2}^{*} \sin \alpha - N_{\phi 2}^{*'} \sin \alpha'\right) \cos 2\theta$, and a shear load $\left(N_{\phi\theta 2}^{*} + N_{\phi\theta 2}^{*'}\right) \sin 2\theta$, positive as shown in figure 29. The two free constants give the opportunity of influencing these forces in such a way that the ring is free of bending. The first thing to do is to make the vertical load vanish at every point. This yields the equation

$$N_{\phi 2}^{*} \sin \alpha - N_{\phi 2}^{*'} \sin \alpha' = 0$$

When the expression just given for $N_{\phi 2}^{*}$ is introduced and some simple geometric relations mentioned before are used, the following equation is obtained:

$$C \frac{\sin \alpha}{(1 - \cos \alpha)^2} - C' \frac{\sin \alpha'}{(1 - \cos \alpha')^2} = 0 \qquad (22a)$$

The second equation in C and C' must express the fact that there is no bending in the plane of the ring. Under this condition the ring has only an axial force F, which, of course, will be a function of θ. From the equilibrium of the ring element (fig. 30) two relations are found:

$$c\left(N_{\phi 2}^{*} \cos \alpha + N_{\phi 2}^{*'} \cos \alpha'\right) \cos 2\theta = F$$

$$c\left(N_{\phi\theta 2}^{*} + N_{\phi\theta 2}^{*'}\right) \sin 2\theta = \frac{dF}{d\theta}$$

From the first one it is possible to write $F = F_2 \cos 2\theta$, and, eliminating F_2 from both equations,

$$N_{\phi 2}^{*} \cos \alpha + N_{\phi 2}^{*'} \cos \alpha' + \frac{1}{2}\left(N_{\phi\theta 2}^{*} + N_{\phi\theta 2}^{*'}\right) = 0$$

When the expressions found for the internal forces of both shells are again introduced and then simplified by appropriate use of geometric relations, this will yield the second equation for C and C':

$$C \frac{(1 - 2 \cos \alpha)}{(1 - \cos \alpha)^2} + C' \frac{(1 - 2 \cos \alpha')}{(1 - \cos \alpha')^2} = \frac{3p(a^2 - b^2)}{b} \frac{\sin (\alpha + \alpha')}{\sin \alpha'} \qquad (22b)$$

These two equations, when solved in general terms, yield

$$C = \frac{3p(a^2 - b^2)}{b} \frac{(1 - \cos \alpha)^2 \sin (\alpha + \alpha')}{\sin \alpha + \sin \alpha' - 2 \sin (\alpha + \alpha')}$$

Introducing this into the formulas for the internal forces, the following expressions for the upper sphere are found:

$$\left.\begin{aligned}
N_{\phi 2}^{*} &= \frac{p(a^2 - b^2)}{2b} \left\{1 + \left[\frac{3 \sin (\alpha + \alpha')}{\sin \alpha + \sin \alpha' - 2 \sin (\alpha + \alpha')}\right] \frac{(1 - \cos \alpha)^2}{(1 + \cos \phi)^2}\right\} \\
N_{\phi\theta 2}^{*} &= -\frac{p(a^2 - b^2)}{2b} \left\{\cos \phi + \left[\frac{3 \sin (\alpha + \alpha')}{\sin \alpha + \sin \alpha' - 2 \sin (\alpha + \alpha')}\right] \frac{(1 - \cos \alpha)^2}{(1 + \cos \phi)^2}\right\} \\
N_{\theta 2}^{*} &= -\frac{p(a^2 - b^2)}{2b} \left\{\cos^2 \phi + \left[\frac{3 \sin (\alpha + \alpha')}{\sin \alpha + \sin \alpha' - 2 \sin (\alpha + \alpha')}\right] \frac{(1 - \cos \alpha)^2}{(1 + \cos \phi)^2}\right\}
\end{aligned}\right\} \qquad (23)$$

These and those in equations (21) are the forces set up in the spherical shell by the fictitious load (20). The last step necessary

is to find from these forces the real forces in the ellipsoidal bulkhead under the uniform air pressure p.

The center of the bulkhead has the coordinates $\phi = 90^\circ$, $\theta = 0^\circ$. The internal forces are here parallel to the yz-plane and, therefore, are the same in the sphere and the ellipsoid:

$$N_\phi = N_{\phi 0}^* + N_{\phi 2}^* \cos 0^\circ$$

$$= \frac{pb}{2} + \frac{p(a^2 - b^2)}{2b}\left\{1 + \frac{\left[3 \sin (\alpha + \alpha')\right](1 - \cos \alpha)^2}{\sin \alpha + \sin \alpha' - 2 \sin (\alpha + \alpha')}\right\}$$

$$= \frac{pa^2}{2b} + \frac{3p(a^2 - b^2)}{2b} \frac{\left[\sin (\alpha + \alpha')\right](1 - \cos \alpha)^2}{\sin \alpha + \sin \alpha' - 2 \sin (\alpha + \alpha')}$$

$$N_\theta = N_{\theta 0}^* + N_{\theta 2}^* \cos 0^\circ$$

$$= \frac{pa^2}{2b} - \frac{3p(a^2 - b^2)}{2b} \frac{\left[\sin (\alpha + \alpha')\right](1 - \cos \alpha)^2}{\sin \alpha + \sin \alpha' - 2 \sin (\alpha + \alpha')}$$

$$N_{\phi\theta} = N_{\phi\theta 0}^* + N_{\phi\theta 2}^* \sin 0^\circ$$

$$= 0$$

On the edge $\theta = \pm 90^\circ$. Here the force N_θ has x-direction and must be reduced by multiplying by $n = b/a$. The force N_ϕ is parallel to the yz-plane; therefore, the forces on corresponding line elements

of sphere and ellipsoid are the same but the line element is reduced in the ratio b/a, hence the force per unit length of this element increased by a factor a/b. The shear is zero. Thus on the edge of the ellipsoid:

$$N_{\phi} = \frac{a}{b}\left(N_{\phi 0}^{*} + N_{\phi 2}^{*} \cos 180^{\circ}\right)$$

$$= \frac{pa}{2} - \frac{pa\left(a^2 - b^2\right)}{2b^2}\left[1 + \frac{3 \sin (\alpha + \alpha')}{\sin \alpha + \sin \alpha' - 2 \sin (\alpha + \alpha')} \frac{(1 - \cos \alpha)^2}{(1 + \cos \phi)^2}\right]$$

$$= \frac{p\left(2b^2 - a^2\right)a}{2b^2} - \frac{3pa\left(a^2 - b^2\right)}{2b^2} \frac{\sin (\alpha + \alpha')}{\sin \alpha + \sin \alpha' - 2 \sin (\alpha + \alpha')} \frac{(1 - \cos \alpha)^2}{(1 + \cos \phi)^2}$$

$$N_{\theta} = \frac{b'}{a}\left(N_{\theta 0}^{*} + N_{\theta 2}^{*} \cos 180^{\circ}\right)$$

$$= \frac{pb^2}{2a} + \frac{p\left(a^2 - b^2\right)}{2a}\left[\sin^2\phi + \cos^2\phi + \frac{3 \sin (\alpha + \alpha')}{\sin \alpha + \sin \alpha' - 2 \sin (\alpha + \alpha')} \frac{(1 - \cos \alpha)^2}{(1 + \cos \phi)^2}\right]$$

$$= \frac{pa}{2} + \frac{3p\left(a^2 - b^2\right)}{2a} \frac{\sin (\alpha + \alpha')}{\sin \alpha + \sin \alpha' - 2 \sin (\alpha + \alpha')} \frac{(1 - \cos \alpha)^2}{(1 + \cos \phi)^2}$$

An example for the distribution of these forces over the circumference is shown in figure 31. In the top and bottom zones the forces are rather uniformly distributed, but there are marked peaks at the junction of the two ellipsoids. This fact indicates that stresses in shells should be determined carefully.

In all the preceding formulas, the denominator

$$\sin \alpha + \sin \alpha' - 2 \sin (\alpha + \alpha')$$

appears. It may happen that α and α' have such values that this denominator is zero, in which case the formulas would yield infinite stresses. This indicates that in such a case the combination of the two spherical or ellipsoidal shells is capable of an inextensional deformation and that rigidity can only be secured by giving the neck ring sufficient rigidity against bending in its own plane. If plane bending of the ring is to be assured, then equation (22a) between the two constants C and C' still must hold. The bending moment in the ring then becomes independent of the choice of C. Equation (22b) becomes useless and must be replaced by the condition that the internal forces assume finite values. This leads to $C = C' = 0$.

The somewhat lengthy analysis of the double bulkhead has been reproduced here not only because of the particular problem under consideration but as an example of two important features of thin shells:

(1) The fact that the stiffening ring along the intersection of two parts of the shell is usually free of bending moments

(2) The use of affine relations for the solution of shell problems

Nose of Plane

General rules.- The nose of the fuselage may have so many various shapes that not much can be said in general about its stress analysis. In high-speed planes aerodynamic consideration may lead to shaping the nose as a perfect surface of revolution. If it is part of the pressurized cabin, it may be treated with formulas (18a) and (18b) for stresses in such shells; if the cabin terminates in a bulkhead back of the nose, all that has been said about the rear bulkhead is applicable.

The modern passenger plane usually has a nose which looks like that shown in figure 32. The major part of it is a shell, but the smooth surface is interrupted by many windows. In such cases a shell analysis as described in the preceding sections will, in general, be too complicated for practical purposes. As regards the stress analysis of such structures, the following facts should be kept in mind:

(1) All large uninterrupted parts of the metal skin will act as shells, whether they are fixed on a solid framework or only stiffened by rings and stringers. The stiffeners which are connected to the shell,

although absolutely necessary for the introduction of local loads and as a buckling reinforcement, are obstructions to a smooth flow of stress in the shell proper and lead to quilting and to tensile stresses in rivets.

(2) All edges of such shell parts, for example, along the windows, must be stiffened by edge members. It is always advantageous to shape these edge members after plane curves. With rare exceptions they will not then be subjected to bending in space, but they must offer resistance to bending in their plane and require the corresponding rigidity, bracing, and support.

(3) There is no need for making cross sections circular. Any curved shell can resist an internal pressure, but, of course, the stress distribution will be less uniform and may easily have local zones of compression if the cross sections are far from circular.

(4) Areas of extremely low curvature should be avoided. Membrane shell theory leads to extremely high stresses in such parts and, owing to these stresses, the panel bulges out, thus increasing the curvature and reducing the stress. In addition this bulging invariably leads to some plastic deformation at the edges of the panel and, therefore, to a permanent bulging, which is undesirable.

Ellipsoid with three different axes.- A general ellipsoid is a kind of a shell which probably will not occur as part of a pressure cabin. However, its membrane forces are easily computed and may give an idea of what may happen in other shells of noncircular cross section.

Consider an ellipsoid having the three half-axes $a > b > c$ and being subjected to an internal pressure p. In order to find the membrane forces, establish relations between them and those in a sphere of radius b under a certain load. This follows the same lines as the theory for the double bulkhead in the section entitled "Bulkhead for Double Cylinders."

In rectangular coordinates x^*, y^*, and z^* the sphere has the equation

$$x^{*2} + y^{*2} + z^{*2} = b^2$$

and in coordinates x, y, and z the equation of the ellipsoid is

$$\frac{x^2}{a^2} + \frac{y^2}{b^2} + \frac{z^2}{c^2} = 1$$

As surface coordinates on the sphere the angles ϕ and θ are used as shown in figure 33. Through the relations

$$x = \frac{a}{b} x^*$$

$$y = y^*$$

$$z = \frac{c}{b} z^*$$

each point of the sphere corresponds to a point on the ellipsoid. By attributing the same values of ϕ and θ to both, a system of coordinates is established on the ellipsoid. Its lines ϕ = Constant are parallel ellipses in horizontal planes. Its lines θ = Constant are ellipses in planes through the z-axis.

The shell element on the sphere has the area

$$dA^* = a\, d\phi a \sin \phi\, d\phi$$

and its projections on the coordinate planes are

$$dA_x^* = dA^* \sin \phi \cos \theta$$

$$dA_y^* = dA^* \sin \phi \sin \theta$$

$$dA_z^* = dA^* \cos \phi$$

The projections of the corresponding element of the ellipsoid are

$$dA_x = \frac{c}{b} dA_x^*$$

$$dA_y = \frac{ac}{b^2} dA_y^*$$

$$dA_z = \frac{a}{b} dA_z^*$$

Multiplying this by p yields the components of the force $p\,dA$ acting on that element. The corresponding forces on the spherical element are then

$$p_x^*\,dA^* = \frac{b}{a}\,p\,dA_x$$

$$= \frac{b}{a}\,p\,\frac{c}{b}\,dA^*\sin\phi\cos\theta$$

$$p_y^*\,dA^* = p\,dA_y$$

$$= p\,\frac{ac}{b}\,dA^*\sin\phi\sin\theta$$

$$p_z^*\,dA^* = \frac{b}{c}\,p\,dA_z$$

$$= \frac{b}{c}\,p\,\frac{a}{b}\,dA^*\cos\phi$$

From these relations are found p_x^*, p_y^*, and p_z^*, the loads per unit area of the sphere, in directions x^*, y^*, and z^*. They are connected with the usual components, X^* in direction θ, Y^* in direction ϕ, and Z^* in the radial direction by the formulas:

$$X^* = -p_x^*\sin\theta + p_y^*\cos\theta$$

$$Y^* = \left(p_x^*\cos\theta + p_y^*\sin\theta\right)\cos\phi - p_z^*\sin\phi$$

$$Z^* = \left(p_x^*\cos\theta + p_y^*\sin\theta\right)\sin\phi + p_z^*\cos\phi$$

Introducing p_x^*, p_y^*, and p_z^*, they yield:

$$X^* = \frac{p}{2}\,\frac{c}{b}\left(\frac{a}{b} - \frac{b}{a}\right)\sin\phi\sin 2\theta$$

$$\equiv X_2\sin 2\theta$$

$$Y^* = \frac{p}{2} \cos \phi \sin \phi \left[\left(\frac{c}{a} + \frac{ac}{b^2} - 2 \frac{a}{c} \right) - \frac{c}{b} \left(\frac{a}{b} - \frac{b}{a} \right) \cos 2\theta \right]$$

$$\equiv Y_o + Y_2 \cos 2\theta$$

$$Z^* = \frac{p}{2} \left[2 \frac{a}{c} + \left(\frac{c}{a} + \frac{ac}{b^2} - 2 \frac{a}{c} \right) \sin^2 \phi - \frac{c}{b} \left(\frac{a}{b} - \frac{b}{a} \right) \sin^2 \phi \cos 2\theta \right]$$

$$\equiv Z_o + Z_2 \cos 2\theta$$

The corresponding membrane forces may be found from well-known formulas (reference 2, pp. 37 to 39). They are:

$$N_\phi^* = \frac{p}{2} \frac{ab}{c} - \frac{pc}{2} \left(\frac{a}{b} - \frac{b}{a} \right) \cos 2\theta$$

$$N_\theta^* = \frac{p}{2} \left[\frac{ab}{c} + \left(\frac{bc}{a} + \frac{ac}{b} - 2 \frac{ab}{c} \right) \sin^2 \phi \right] + \frac{pc}{2} \left(\frac{a}{b} - \frac{b}{a} \right) \cos^2 \phi \cos 2\theta$$

$$N_{\phi\theta}^* = \frac{pc}{2} \left(\frac{a}{b} - \frac{b}{a} \right) \cos \phi \sin 2\theta$$

To find the forces in the ellipsoid, the ratio of the corresponding line elements is needed. The results are mentioned only for the three points A, B, and C.

At the point A $\phi = 90^\circ$, $\theta = 0^\circ$, and

$$N_\phi = \frac{pa}{2} - \frac{pc^2}{2b} \left(\frac{a}{b} - \frac{b}{a} \right)$$

$$= \frac{p}{2} \left(a - \frac{ac^2}{b^2} + \frac{c^2}{a} \right)$$

$$= \frac{pa}{2} \left(1 - \frac{c^2}{b^2} + \frac{c^2}{a^2} \right)$$

$$N_\theta = \frac{pb}{2c}\left(\frac{bc}{a} + \frac{ac}{b} - \frac{ab}{c}\right)$$

$$= \frac{p}{2}\left(\frac{b^2}{a} + a - \frac{ab^2}{c^2}\right)$$

$$= \frac{pa}{2}\left(1 - \frac{b^2}{c^2} + \frac{b^2}{a^2}\right)$$

At the point B $\phi = 90^\circ$, $\theta = 90^\circ$, and

$$N_\phi = \frac{pb}{2}\left(1 + \frac{c^2}{b^2} - \frac{c^2}{a^2}\right)$$

$$N_\theta = \frac{pb}{2}\left(1 + \frac{a^2}{b^2} - \frac{a^2}{c^2}\right)$$

At the point C $\phi = 0^\circ$ and θ may have any value. When $\theta = 0^\circ$ is assumed arbitrarily, then N_ϕ lies in the xz-plane, and N_θ, in the yz-plane, and the internal forces are:

$$N_\phi = \frac{pc}{2}\left(1 - \frac{a^2}{b^2} + \frac{a^2}{c^2}\right)$$

$$N_\theta = \frac{pc}{2}\left(1 - \frac{b^2}{a^2} + \frac{b^2}{c^2}\right)$$

If $(a^2 + b^2)c^2 < a^2b^2$, the force N_θ at the points A and B becomes a compression. The other four formulas always yield positive forces when $a \geqq b \geqq c$. These results may serve as a first orientation of what is to be expected in shells of noncircular cross section under the action of an internal pressure.

PLATE PROBLEMS

Stresses in Thin Flat Sheets

Plane plates are not very desirable as parts of the wall of a pressure vessel, but it often is not possible to avoid them. Therefore, the stresses set up in them by a lateral pressure p will be considered here.

If such a plate were thick enough, it might carry its load by bending stresses as does the reinforced concrete floor slab of a building; however, the skin of an airplane is much too thin to carry an appreciable load with tolerable bending stresses. Its stress system is a superposition of bending stresses and of the stresses in a flexible skin.

The subject of this section will be such a thin skin of rectangular shape. Its stress problem is essentially nonlinear. In two dimensions it is so involved that all theoretical and experimental effort spent on it up to the present is still far from giving a complete answer to all questions which the engineer might ask. Therefore, a discussion is first presented for the one-dimensional problem which, in many cases, will give useful information for practical purposes and beyond that will show the general features of the stress system present in the two-dimensional case.

Thin sheet stressed in one dimension.- Consider a thin plate as shown in figure 34. In the x-direction it has the span l, and the sides $x = \pm l/2$ are supported in such a way that not only the deflection w but also a displacement u in the x-direction is prohibited. In the direction of the y-axis the plate is supposed to be long enough to make the conditions at the shorter sides immaterial.

For the purpose of stress analysis cut a strip of unit width out of this plate. Because of the end conditions, the lateral load p will produce a direct stress σ along the strip, which is necessarily independent of x. If the deflection w is large enough, this stress will be capable of carrying the load.

This can be seen on an element of length dx cut from the strip (fig. 35). The condition of vertical equilibrium is:

$$\sigma t\, d\left(\frac{dw}{dx}\right) + p\, dx = 0$$

It yields the relation

$$\frac{d^2w}{dx^2} = - \frac{p}{\sigma t}$$

which indicates that the strip must deflect into a common parabola:

$$w = \frac{p l^2}{8\sigma t}\left(1 - \frac{4x^2}{l^2}\right)$$

with a maximum at $x = 0$:

$$f = \frac{p l^2}{8\sigma t} \tag{24}$$

The horizontal displacement in the direction of increasing x may be called u. The strain in the strip is then

$$\epsilon = \frac{du}{dx} + \frac{1}{2}\left(\frac{dw}{dx}\right)^2$$

$$= \frac{\sigma}{E}$$

At the center $x = 0$, $u = 0$ from symmetry. At the support $x = l/2$, therefore,

$$u = u_o$$

$$= \frac{\sigma}{2E} - \frac{1}{2}\int_0^{l/2} \left(\frac{dw}{dx}\right)^2 dx$$

$$= \frac{\sigma l}{2E} - \frac{p^2 l^3}{48\sigma^2 t^2} \tag{25}$$

Since an unyielding support $u_o = 0$ was assumed, this equation may be used to find σ for a given load:

$$\sigma = \frac{1}{2}\sqrt[3]{\frac{E p^2 l^2}{3t^2}}$$

From equation (24) the final expression for the deflection may be found, in particular that for the maximum $w = f$ at $x = 0$:

$$f = \frac{l}{4}\sqrt[3]{\frac{3pl}{Et}}$$

These two formulas represent nonlinear relations, owing to the quadratic term which represents the influence of the deflection w on the strain ϵ. If this term should be neglected, as it is in many other cases, no reasonable result at all would be reached. The nonlinearity is, therefore, an essential feature of this problem.

Since the plate deflects, there will be a bending moment

$$M = -EI\frac{d^2w}{dx^2}$$

$$= E\frac{t^3}{12}\frac{p}{\sigma t}$$

$$= \frac{t^2}{6}\sqrt[3]{\frac{3E^2pt^2}{l^2}}$$

This is incompatible with the assumed support and has been neglected in the preceding formulas, but this may safely be done if M is small as compared with the moment $pl^2/8$ which would be necessary to carry the load by beam action. This condition may be brought into the dimensionless form:

$$\frac{Et^4}{pl^4} \ll \frac{3}{16}$$

For a pressure cabin with $p = 7$ psi and duralumin with $E = 10^7$ psi this yields

$$\frac{t}{l} \ll \frac{1}{50}$$

For the airplane, the assumption of unyielding supports goes too far. The edges $x = \text{Constant}$ of the plate are kept apart by stiffeners in the x-direction. When they are not riveted to the skin, the problem is still one-dimensional and may be represented by a flexible strip and

a strut as shown in figure 36. The flexible strip is exposed to the load p and deflects under it; its ends are kept apart by a strut of cross section A_1, which has a compressive force $N = -\sigma t$; the supports are such that they allow the corresponding elastic deformation of the bar.

When the cross section of one stiffener is A, and the distance between stiffeners is d, then the area $A_1 = A/d$ corresponds to a strip of unit width of the plate.

When the horizontal displacement u is assumed to be zero at $x = 0$ (midspan), equation (25) may again be used for the displacement u_o at the end, but now u_o must correspond to the fact that the strut becomes shorter by Nl/EA_1:

$$u_o = -\frac{\sigma t l}{2EA_1}$$

Introducing this into equation (25),

$$\sigma = \frac{1}{2}\sqrt[3]{\frac{Ep^2l^2}{3t^2}}\sqrt[3]{\frac{A_1}{A_1 + t}} \tag{26a}$$

for the stress in the plate. The greatest deflection follows then from equation (24):

$$f = \frac{l}{4}\sqrt[3]{\frac{3pl}{Et}}\sqrt[3]{1 + \frac{t}{A_1}} \tag{26b}$$

Comparing these two formulas with those which were obtained for nonyielding supports, it is seen that they become identical for $A_1 \longrightarrow \infty$. Since t/A_1 is more likely to be equal to 1 than 0, the assumption of nonyielding supports may lead to errors of about 25 percent, overrating the stress and underrating the deflection. It seems, therefore, not worth while to spend much effort on the two-dimensional problem if this effect is not taken into account. However, the simpler formulas are good enough for estimating the order of magnitude of σ and f and for discussing the influence of the bending stiffness of the plate.

The formulas (26a) and (26b) are sufficient if the sheet panel is part of a flat bulkhead. But in most other cases the wall, consisting of the sheet and its stiffeners, has to transmit an internal force such

as N_x or N_ϕ explained in the section entitled "Circular Cylinder." These forces may be due to the over-all bending of the fuselage, to the action of the internal pressure on other parts of its wall, and to other causes. When the sheet is flat and bulges out, the distribution of this force on sheet and stiffeners is no longer governed by the formulas (5). It may be found by adding an axial force P to the strip and strut system of figure 36 (see fig. 37).

If σ again indicates the stress in the sheet, the force in the strut is

$$N = P - \sigma t$$

and the horizontal displacement at $x = l/2$ must be

$$u_o = \frac{Nl}{2EA_1}$$

Equating this to the expression (25),

$$\sigma^3\left(1 + \frac{t}{A_1}\right) - \sigma^2 \frac{P}{A_1} - \frac{Ep^2l^2}{24t^2} = 0 \qquad (27)$$

This may easily be solved in any given case. The deflection f follows then from equation (24).

Some results are shown in figure 38 in dimensionless variables. The values for the parameter pl/Et have been chosen as rather extreme in order to cover the whole field of practical interest. For most of the diagrams, $t/A_1 = 1$ has been assumed, but one of them shows the trend for a variation of this parameter.

The diagrams show the influence of the force P. They emphasize that a solution of the two-dimensional problem which disregards this influence cannot yield more than a rough approximation of the real airplane problem, even if it were an exact solution of the simplified problem.

Thin sheet stressed in two dimensions.- Assuming a sufficiently thin plate, the formulas developed in the preceding section are exact for infinitely long rectangles. It is probable that they will yield good results if the ratio of the sides is 1:4 or even 1:3, but when the rectangle approaches a square, they become inapplicable.

To find out how the results must be modified in such cases, consider a square plate framed by four equal stiffeners (fig. 39). When the plate bulges out under a lateral load p, stresses σ will be set up in two directions, which are denoted σ_x and σ_y. The stiffeners will receive compressive forces. The plate in their immediate vicinity must have the same strain and hence a compressive stress. The distribution of σ_y along one of the edges must, therefore, be as shown on the figure.

At the center of the plate $\sigma_x = \sigma_y$. When two strips are cut out along the coordinate axes, each one will carry one-half of the load p, and the curvature will be half of that which would follow with this same σ from the one-dimensional theory. When the horizontal strip is followed toward the right edge of the plate, the stress σ_y will decrease and finally become negative. Where it passes zero, the one-dimensional theory will yield the correct curvature, and closer to the edge the curvature of the square plate will be greater than that of a single strip. A single strip was seen to deflect as a parabola. The profile of the square plate must, therefore, be far from a sine curve, and results computed on this assumption must, therefore, be interpreted with some reserve.

When a diagonal of the plate is followed σ_x always equals σ_y, but both stresses decrease the father away they are from the center. The curvature in both directions must, therefore, become greater, and a sharp fold may be expected toward the corner. But at least there is a region where σ_x and σ_y become negative and are no longer capable of carrying any load at all. Here even the thinnest plate must have essential bending stress. The thinner the plate is, the smaller this region will be, and the sharper the curvature will become. It follows that the highest stresses will occur on or near the corners. They may or may not be responsible for the ultimate load of the plate, depending on the possibility of smoothening the peak by local plastic flow, but they are certainly responsible for permanent deformations which produce that quilting of flat panels which makes airplanes unsightly and is not much appreciated by the aerodynamicist.

There is little numerical information available on square and rectangular plates. Some papers (references 6 and 10) are mentioned in the references of this report. One of them, reference 6, contains rather complete material for plates with unyielding supports (fig. 34); however, this paper is based on the assumption that the profiles of the deflected plate along both axes are sine curves. In particular, this assumption is also made for the lengthwise profile of long plates (1:4), where it leads to an overrating of the influence of the support at the short sides. The results for the long plate, therefore, do not check with the one-dimensional theory. However, the two-dimensional problem is

so complex that a critical use of the diagrams of Moness (reference 6) is the best that can be recommended at this time.

Thermal Stresses in Window Panes

The window panes of a pressure cabin are not only exposed to the difference in pressure between the interior of the cabin and the free atmosphere but also to a considerable difference in temperature. The bending stresses due to the pressure may easily be found from textbook formulas, but the thermal stresses require some discussion.

Consider a plate of uniform thickness, simply supported along its edge. Assume that no load is applied but that there is a difference T between the temperatures of its faces. When the temperature is increased by T, a positive strain

$$\epsilon = \alpha T$$

will occur in every direction, α being the coefficient of thermal expansion. When only one side of the plate is heated, ϵ is the difference in strain between both sides, and this difference leads to a curvature

$$\kappa = \frac{\epsilon}{t} = \frac{\alpha T}{t}$$

in every direction. The middle surface of the plate is then deformed into a small part of a sphere of radius $1/\kappa$.

If the plate is circular, this is all that happens. The window will slightly deflect to the warmer side, and no thermal stresses will be set up. But if the plate is rectangular, the deformed shape will no longer fit on the support, and, in order to make it fit, the support will exert forces on the plate and these forces will produce bending stresses.

Formulas for the bending moments which correspond to these stresses will now be established and discussed. In doing so, the following notations will be used (fig. 40):

x,y	coordinates
w	deflection
M_x,M_y	bending moments
M_{xy}	twisting moment

κ_x curvature in x-direction $\left(\frac{\partial^2 w}{\partial x^2}\right)$

K bending stiffness $\left(\frac{Et^3}{12(1 - \nu^2)}\right)$

The stresses and deformation due to heating of the upper face of the plate will be built up in three steps. The first one has already been done, namely, the application of the temperature difference to the free plate, resulting in a uniform bending without stress.

In the second step this deformation is completely removed by applying, along all four edges of the plate, constant external bending moments M_o of appropriate size. They produce bending moments

$$M_x = M_y = M_o$$

in the plate which are constant everywhere and in all directions. Now, the curvature κ_x of the plate is related to the bending moment by the well-known formula:

$$\kappa_x = -\frac{1}{K(1 - \nu^2)}(M_x - \nu M_y)$$

In this case, it yields

$$\kappa_x = -\frac{M_o}{K(1 + \nu)}$$

To remove the thermal deformation, κ_x must be made equal to $-\alpha T/t$ and therefore

$$M_o = K(1 + \nu)\frac{\alpha T}{t}$$

Under the combined action of the temperature T and the edge moments M_o the plate is perfectly plane and may be attached to its supports. Now the third step may be done: The condition of simply supported edges must be realized and the edge load M_o compensated by

adding an edge load $-M_o$. This is a problem of plate theory and may be solved in the following way:

When there is no lateral load, the deflection w of the plate must satisfy the well-known differential equation (reference 11):

$$\frac{\partial^4 w}{\partial x^4} + 2\frac{\partial^4 w}{\partial x^2 \partial y^2} + \frac{\partial^4 w}{\partial y^4} = 0$$

Introducing the sum of the two bending moments

$$M = M_x + M_y$$

as an auxiliary variable, this equation may be split into two equations of the second order:

$$\frac{\partial^2 M}{\partial x^2} + \frac{\partial^2 M}{\partial y^2} = 0 \tag{28a}$$

$$\frac{\partial^2 w}{\partial x^2} + \frac{\partial^2 w}{\partial y^2} = -\frac{M}{K(1 + \nu)} \tag{28b}$$

These equations can be solved one after the other because a boundary condition can be found for each one.

Consider, for example, the edge $x = a/2$ of the rectangle. The bending moment $-M_o$ is applied there and

$$M_x = -M_o$$

is obtained. Since the edge is supported, $w = 0$ for all values of y and, hence, also

$$\frac{\partial^2 w}{\partial y^2} = 0$$

Introducing this into the elastic law

$$\left.\begin{aligned} M_x &= -K\left(\frac{\partial^2 w}{\partial x^2} + \nu \frac{\partial^2 w}{\partial y^2}\right) \\ M_y &= -K\left(\frac{\partial^2 w}{\partial y^2} + \nu \frac{\partial^2 w}{\partial x^2}\right) \end{aligned}\right\} \tag{29}$$

it can be concluded that $M_y = -\nu M_o$ on this edge and, hence, that

$$M = -(1 + \nu)M_o \tag{30}$$

A similar reasoning may be made for the three other edges.

The solution of equation (28a) with the boundary condition (30) is extremely simple. It is a constant, $M = -(1 + \nu)M_o$.

Now equation (28b) may be attacked. Introducing the result just obtained,

$$\frac{\partial^2 w}{\partial x^2} + \frac{\partial^2 w}{\partial y^2} = \frac{M_o}{K}$$

and the boundary condition is, of course, $w = 0$.

This differential equation with this boundary condition is known in the theory of torsion of a bar having rectangular cross section. All that is necessary is to translate the solution known there into the terminology of the plate problem.

The solution is:

$$w = \frac{M_o}{K}\left(-\frac{b^2}{8} + \frac{y^2}{2} + \frac{4b^2}{\pi^3} \sum_{1,3,5,\ldots}^{\infty} (-1)^{\frac{n-1}{2}} \frac{\cosh \frac{n\pi x}{b} \cos \frac{n\pi y}{b}}{n^3 \cosh \frac{n\pi a}{2b}}\right) \tag{31}$$

One may easily verify that this expression satisfies the differential equation and that $w = 0$ for $y = \pm b/2$. At the other two edges, $x = \pm a/2$, equation (31) yields:

$$w = \frac{M_o}{K}\left(-\frac{b^2}{8} + \frac{y^2}{2} + \frac{4b^2}{\pi^3}\sum_{1,3,5,\ldots}^{\infty}(-1)^{\frac{n-1}{2}}\frac{1}{n^3}\cos\frac{n\pi y}{b}\right)$$

The sum in the parentheses happens to be the Fourier series representation of the function

$$\frac{\pi^2}{4b^2}\left(\frac{b^2}{8} - \frac{y^2}{2}\right)$$

valid in the interval $-b/2 \leqq y \leqq b/2$, and, therefore, the expression in parentheses vanishes at every point of the two edges x = Constant of the plate. This proves that the solution really satisfies the condition $w = 0$ on all four sides of the rectangle.

The bending moments can now be found easily by introducing the solution (31) into the elastic law (29):

$$M_x = -M_o\left[\nu + \frac{4(1-\nu)}{\pi}\sum_{1,3,\ldots}^{\infty}(-1)^{\frac{n-1}{2}}\frac{\cosh\frac{n\pi x}{b}\cos\frac{n\pi y}{b}}{n\cosh\frac{n\pi a}{2b}}\right]$$

$$M_y = -M_o\left[1 - \frac{4(1-\nu)}{\pi}\sum_{1,3,\ldots}^{\infty}(-1)^{\frac{n-1}{2}}\frac{\cosh\frac{n\pi x}{b}\cos\frac{n\pi y}{b}}{n\cosh\frac{n\pi a}{2b}}\right]$$

These are the bending moments produced in step three. To obtain the bending moments for the original problem, the moment M_o of the second step must be added; the first step makes no contribution to the stresses. When M_o is expressed by the temperature difference T, writing

$$M_o = K(1 + \nu)\frac{\alpha T}{t}$$

$$= \frac{E\alpha t^2 T}{12(1 - \nu)}$$

finally

$$M_x = \frac{1}{3\pi} E\alpha t^2 T \left[\frac{\pi}{4} - \sum_{1,3,\ldots}^{\infty} (-1)^{\frac{n-1}{2}} \frac{\cosh \frac{n\pi x}{b} \cos \frac{n\pi y}{b}}{n \cosh \frac{n\pi a}{2b}} \right]$$

$$M_y = \frac{1}{3\pi} E\alpha t^2 T \sum_{1,3,\ldots}^{\infty} (-1)^{\frac{n-1}{2}} \frac{\cosh \frac{n\pi x}{b} \cos \frac{n\pi y}{b}}{n \cosh \frac{n\pi a}{2b}}$$

The solution would not be complete without having the twisting moment M_{xy}. Step two does not make a contribution to it, but it can be obtained from equation (31) alone, using the formula

$$M_{xy} = -K(1 - \nu) \frac{\partial^2 w}{\partial x \, \partial y}$$

There is obtained

$$M_{xy} = \frac{1}{3\pi} E\alpha t^2 T \sum_{1,3,\ldots}^{\infty} (-1)^{\frac{n-1}{2}} \frac{\sinh \frac{n\pi x}{b} \sin \frac{n\pi y}{b}}{n \cosh \frac{n\pi a}{2b}}$$

The formulas for the moments are the solution of the problem as it was formulated at the beginning. It is now necessary to discuss this result and to draw some practical conclusions from it.

At the edges $y = \pm b/2$

$$\cos \frac{n\pi y}{b} = 0$$

for all odd integers n and hence

$$M_x = \frac{1}{12} E\alpha t^2 T$$

$$M_y = 0$$

That the moment M_y vanishes corresponds to the assumed simple support. That M_x does not do so is due to the fact that the edge is kept straight in spite of the applied temperature difference.

At the edges $x = \pm a/2$ there is the corresponding result

$$M_x = 0$$

$$M_y = \frac{1}{12} E\alpha t^2 T$$

but to obtain it the Fourier series

$$\sum_{1,3,\ldots}^{\infty} (-1)^{\frac{n-1}{2}} \frac{1}{n} \cos \frac{n\pi y}{b}$$

must be added up which yields $\pi/4$ for all points of the interval $-b/2 \leqq y \leqq b/2$.

For interior points of the plate, the series appearing in the formulas M_x and M_y has very good convergence. For the center of a square plate,

$$M_x = M_y$$

$$= \frac{1}{24} E\alpha t^2 T$$

can be found easily.

The most interesting part of the solution is the formula for the twisting moment M_{xy}. When $x < a/2$, the quotient of the two hyperbolic functions decreases exponentially with increasing n and produces a good convergence of the series; but on the edge $x = a/2$ this beneficial influence is lost and the series converges slowly. If $x = a/2$ is kept and the corner $y = b/2$ is approached, the series becomes

$$\sum_{1,3,\ldots}^{\infty} (-1)^{\frac{n-1}{2}} \frac{1}{n} \sin \frac{n\pi}{2} = \sum_{1,3,\ldots}^{\infty} \frac{1}{n}$$

and this series is divergent or, if this expression is admitted, yields the value ∞. This singularity of the twisting moment which, of course, appears at all four corners, is of practical importance. It is true that real objects always find a way to avoid infinite stresses. Here the finite thickness of the plate, the finite width of the zone to which the reactions are applied, and the elastic yielding of the support may act in this way, but, nevertheless, the singularity in our solution reveals the fact that stresses near the corner will be extremely high and that it would be wiser to round the corners liberally than to trust the good will of the structure.

Buckling of Cylindrical Panel

The metal skin of the pressurized cabin is subdivided into rectangular panels by rings and axial stiffeners (stringers). In every such panel, the wall is subjected to a hoop stress σ_ϕ due to the cabin pressure p. Additionally, there may be an axial stress σ_x (tension or compression) and a shear stress τ (fig. 41). The hoop stress σ_ϕ increases the shear stress τ required for buckling in the presence of a given σ_x.

For this buckling problem, Kromm (reference 7) has worked out two diagrams which give the critical shear τ as a function of the hoop stress σ_ϕ assuming either $\sigma_x = 0$ (case "a", fig. 43(a)) or $\sigma_x = \sigma_\phi/2$ (case "b", fig. 43(b)). Of course, the ratio between the two stresses σ_x and σ_ϕ may have any other value between or beyond these limits, but, since the influence of σ_x on the critical shear is not large, the choice made by Kromm is sufficient.

Kromm's paper gives only a short description of the method used for solving the problem, referring for more details to his earlier papers on

stability problems in cylinders. A still shorter outline will be given here of the laborious procedure and an explanation of the diagrams resulting from it.

The object of the graphs is a rectangular panel, cut from a circular cylinder of radius a and supported on its edges. Its length is supposed to be much greater than its width so that the buckling is not influenced much by the support on the curved sides.

When this panel is subjected to the cabin pressure p it will bulge out, again forming a cylindrical surface, but with a smaller radius $r < a$. This radius r may easily be found if the lengthwise edges of the panel are fixed. In the deformed state (fig. 42) a simple consideration of equilibrium yields for the hoop stress the relation

$$\sigma_{\phi} = \frac{pr}{t} \tag{32}$$

On the other hand, the length of the arc of radius r and chord b is

$$l = b\left(1 + \frac{b^2}{24r^2}\right)$$

the length of the same arc before deformation is

$$l_o = b\left(1 + \frac{b^2}{24a^2}\right)$$

and hence the hoop strain is

$$\epsilon_{\phi} = \frac{l - l_o}{b}$$

$$= \frac{b^2}{24}\left(\frac{1}{r^2} - \frac{1}{a^2}\right)$$

When $\sigma_x = 0$ (case "a"),

$$\sigma_{\phi} = E\epsilon_{\phi}$$

$$= \frac{Eb^2}{24}\left(\frac{1}{r^2} - \frac{1}{a^2}\right)$$

Equating this to the value from equation (32),

$$\frac{p}{E} = \frac{tb^2}{24} \frac{1}{r}\left(\frac{1}{r^2} - \frac{1}{a^2}\right)$$

In case "b," E has simply to be replaced by $2E/(2 - \nu)$.

In connection with the buckling problem, the relations between p and r must be expressed by a certain set of dimensionless variables used there. Using Kromm's notation, the curvature of the undeformed cylinder is described by the parameter

$$\omega_o = \frac{12(1 - \nu^2)}{\pi^4} \frac{b^4}{a^2 t^2} \tag{33}$$

that of the deformed shell, by

$$\omega_o = \frac{12(1 - \nu^2)}{\pi^4} \frac{b^4}{r^2 t^2}$$

and the pressure p, by the parameter

$$k_p = \frac{p}{E}\left(1 - \nu^2\right)^{3/2} \frac{b^4}{t^4} \tag{34}$$

The relation just found between p and r reads then in case "a":

$$\sqrt{\omega}\left(\omega - \omega_o\right) = 576 \frac{\sqrt{3}}{\pi^6} k_p$$

$$= 1.035 k_p$$

and in case "b":

$$\sqrt{\omega}\left(\omega - \omega_o\right) = \left(1 - \frac{\nu}{2}\right) 576 \frac{\sqrt{3}}{\pi^6} k_p$$

$$= 0.880 k_p$$

After this preparation, the buckling problem for a cylinder of radius r may be solved. This may be done by either of the two standard methods. The differential equations for the components u, v, and w of the displacement may be formulated and solved, or the expression for the variation of the potential energy may be established and equated to zero for every possible variation u, v, or w of the displacements compatible with the boundary conditions. In both cases the displacements are introduced as double Fourier series, and the buckling condition finally assumes the form that a determinant of infinite order must be equal to zero. For the numerical evaluation, this determinant is approached by a section of moderate size, not necessarily situated at its upper left corner. The diagrams in figures 43(a) and 43(b) have been computed in this way.

For the application of these diagrams, it is necessary to know the boundary conditions assumed. Since the plate was supposed to be long in the x-direction, no conditions were fixed for the curved edges x = Constant. On the straight edges, four conditions must be given. The following choice was made: Displacement parallel to the edge $u = 0$, radial displacement $w = 0$, clamping moment (see fig. 8) $M_\phi = 0$, and additional hoop stress $\sigma_\phi = 0$.

The first three of these conditions appear to be reasonable at first sight. Also the last one is quite usual in buckling problems of this kind, but it seems to contradict the assumption of unyielding supports made for the determination of r. This contradiction may be easily resolved. The underlying idea is that the panel is part of the wall of a cylindrical fuselage and has many neighbors which are in the same situation. When the pressure p is applied to these panels, they will all develop the same hoop stress σ_ϕ. Although the stringers usually have but little bending stiffness, they cannot deflect in the v-direction (fig. 41), because the forces $\sigma_\phi t$ applied to them from both sides are in equilibrium. When buckling occurs, the situation is quite different. A system of folds is formed in each panel, and with them additional hoop stresses σ_ϕ are set up. If the stringer were very stiff, corresponding forces $\sigma_\phi t$ would be transmitted to it, and they would not be the same from both sides but would pull at some places to one side and at other places to the other side. When the stringer is weak, as is usual, it will deflect so much that the stresses become almost zero, and the safest assumption for the determination of the buckling stress is the one made.

The use of the diagrams may now be described. From the given data $\sqrt{\omega_0}$ and k_p are computed according to equations (33) and (34) and located in the diagram. The values k_p are found at the left side of

the graph and refer to the more-or-less horizontal curves. For $\sqrt{\omega_0}$, some values are given along the upper edge. The curves to which they refer are almost vertical and join at their lower end, more or less tangentially, a vertical line bearing the same number on the $\sqrt{\omega}$ scale. From this relation it is easy to interpolate more curves $\sqrt{\omega_0}$ and to find the values $\sqrt{\omega_0}$ for those curves which are not numbered in the graph. It also appears that in the right-hand half of the diagram the $\sqrt{\omega_0}$ curves are practically identical with the vertical coordinate lines.

From the point which corresponds to the given values of k_p and $\sqrt{\omega_0}$ follow a horizontal line toward the left and read there τ/σ^*. When multiplied by the reference stress

$$\sigma^* = \frac{\pi^2}{3} \frac{E}{1 - \nu^2} \frac{t^2}{b^2}$$

it yields the critical value of the shear stress τ.

If, incidentally, σ_x corresponds to one of the two cases "a" or "b," it is necessary to consult only one of the diagrams. For other values of σ_x it is necessary to use both and then find the final value τ by interpolation. Since the influence of σ_x is not great, even an extrapolation will be possible, within moderate limits.

Stanford University
Stanford, Calif., September 7, 1950

REFERENCES

1. Köller, Hermann: Spannungsverlauf und mittragende Breite bei Lasteinleitung in orthotrope Blechscheiben. Jahrb. 1940 deutschen Luftfahrtforschung, Bd. I, pp. 852-860.

2. Flügge, W.: Statik und Dynamik der Schalen. Julius Springer (Berlin), 1934.

3. Flügge, W.: Stresses in Shells. (To be published by the McGraw-Hill Book Co., Inc., in 1952.)

4. Schorer, H.: Line Load Action on Thin Cylindrical Shells. Proc. Am. Soc. Civ. Eng., vol. 61, March 1935, pp. 281-316.

5. Flügge, W., and Tschech, E.: Statik der Höhenkammern. Forschungsbericht Nr. 1213, DVL, May 3, 1940.

6. Moness, Elias: Flat Plates under Pressure. Jour. Aero. Sci., vol. 5, no. 11, Sept. 1938, pp. 421-425.

7. Kromm, A.: Beulfestigkeit von versteiften Zylinderschalen mit Schub und Innendruck. Jahrb. 1942 deutschen Luftfahrtforschung, Bd. I, pp. 596-601.

8. Flügge, W.: Schalenstatik und Höhenkammer. Bericht 126, Lilienthal-Gesellschaft für Luftfahrtforschung, 1940, pp. 3-14.

9. Howland, W. L., and Beed, C. F.: Test of Pressurized Cabin Structures. Jour. Aero. Sci., vol. 8, no. 1, Nov. 1940, pp. 17-23.

10. Neubert, M., and Sommer, A.: Rechteckige Blechhaut unter gleichmässig verteiltem Flüssigkeitsdruck. Luftfahrtforschung, Bd. 17, Nr. 7, July 20, 1940, pp. 207-210.

11. Timoshenko, S.: Theory of Plates and Shells. First ed., McGraw-Hill Book Co., Inc., 1940, pp. 99-100.

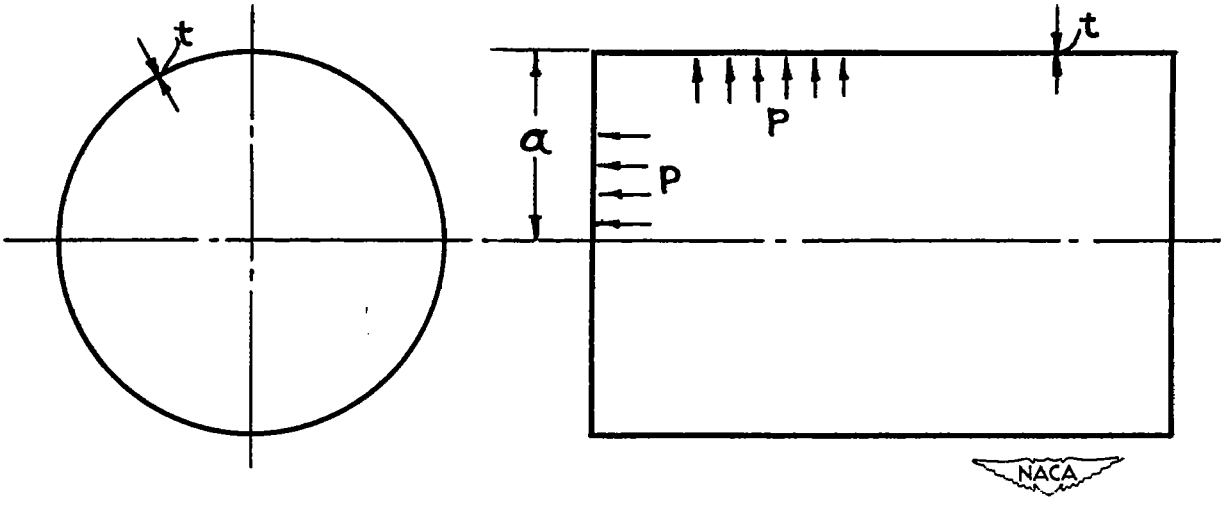

Figure 1.- Cylindrical shell.

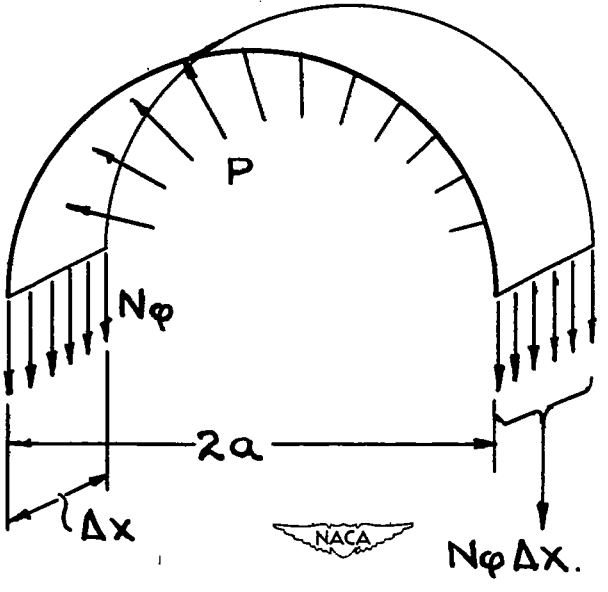

Figure 2.- Part cut from a cylindrical shell subjected to internal pressure p.

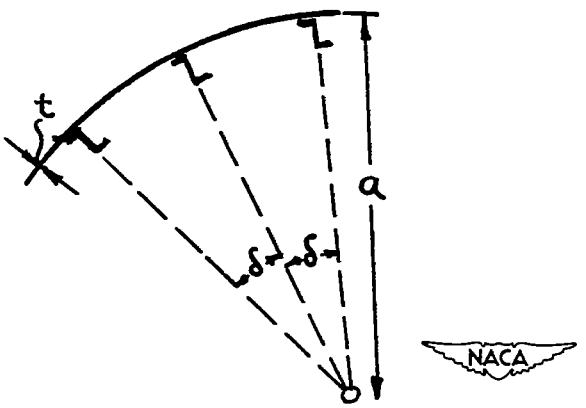

Figure 3.- Part of cross section through a cylindrical shell with stringers.

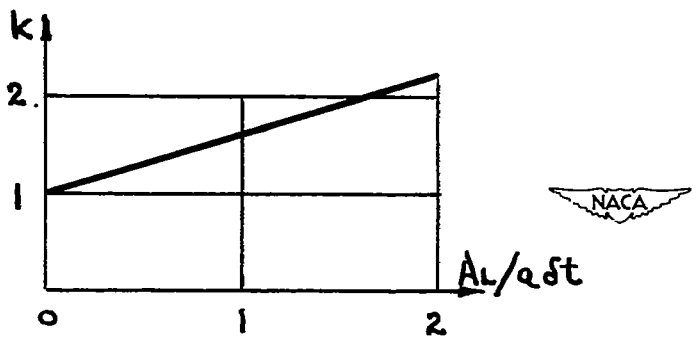

Figure 4.- Factor k for longitudinal stress in skin of stiffened shell.

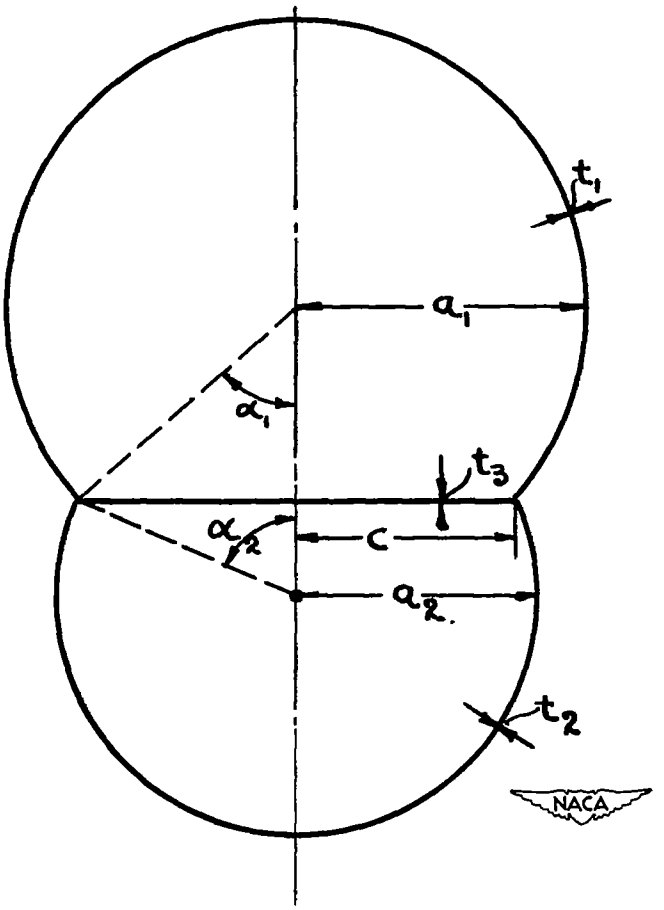

Figure 5.- Cross section through a pressurized cabin consisting of two cylindrical shells.

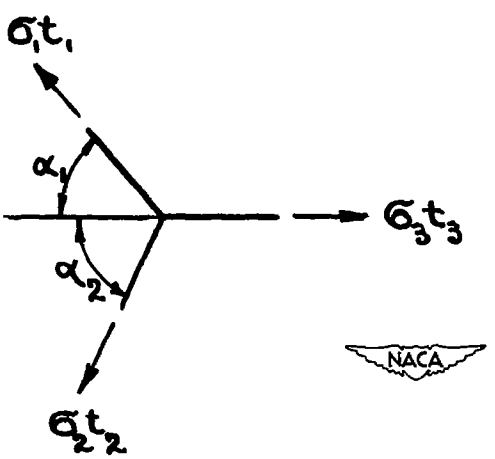

Figure 6.- Detail of figure 5: Forces at junction of two cylinders.

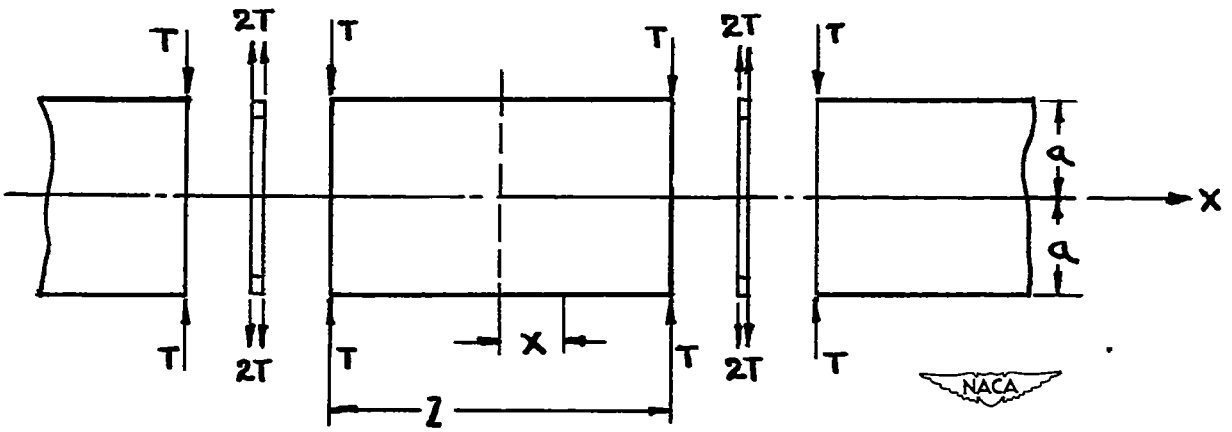

Figure 7.- Longitudinal section through cylindrical shell and reinforcing rings.

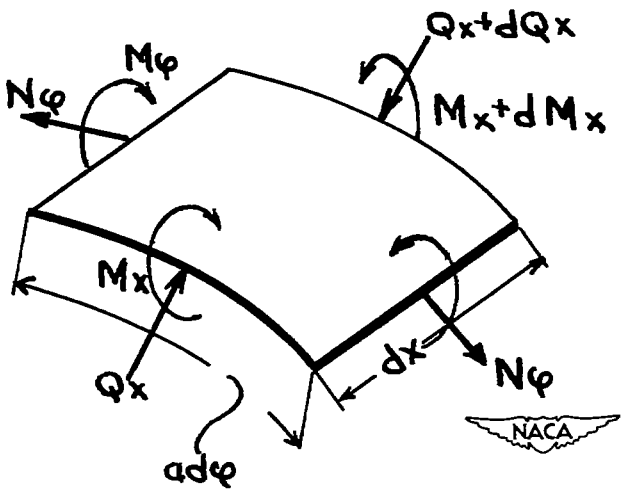

Figure 8.- Element of cylindrical shell, showing internal forces.

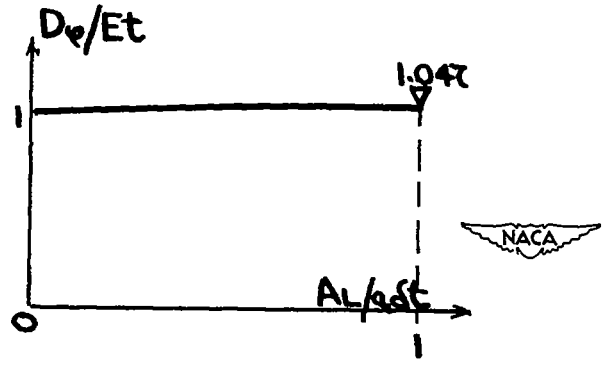

Figure 9.- Extensional rigidity of shell against cross section of stringers.

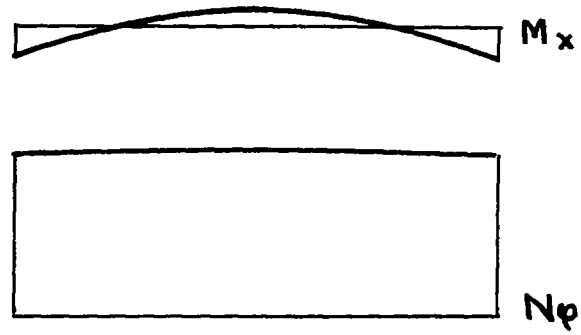

(a) Closely spaced rings, heavy stringers.

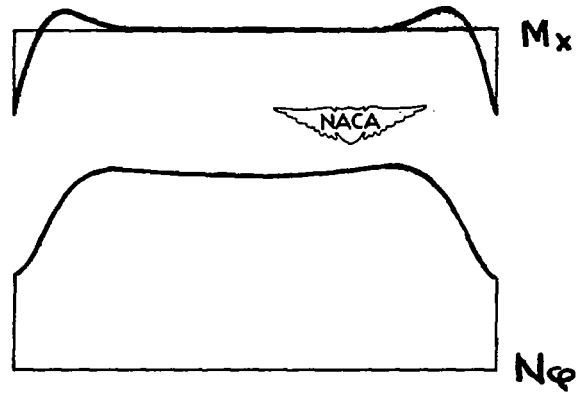

(b) Rings far apart, light stringers.

Figure 10.- Typical distribution of bending moment M_x and hoop force N_ϕ in shell between two rings.

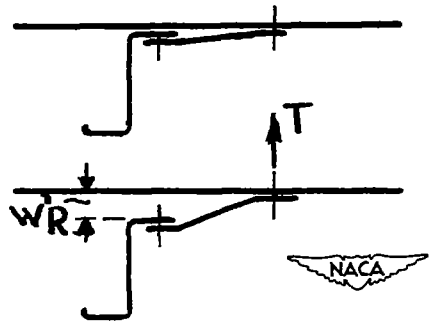

Figure 11.- Yielding connection between shell and ring.

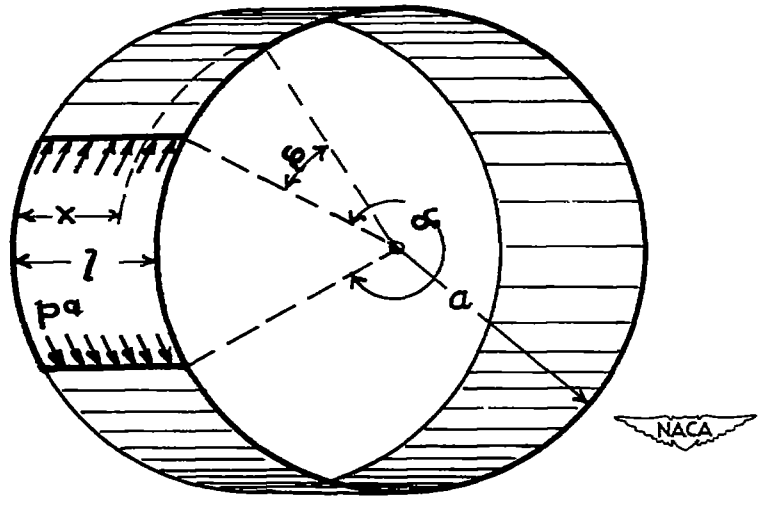

Figure 12.- Cylindrical shell having a door opening.

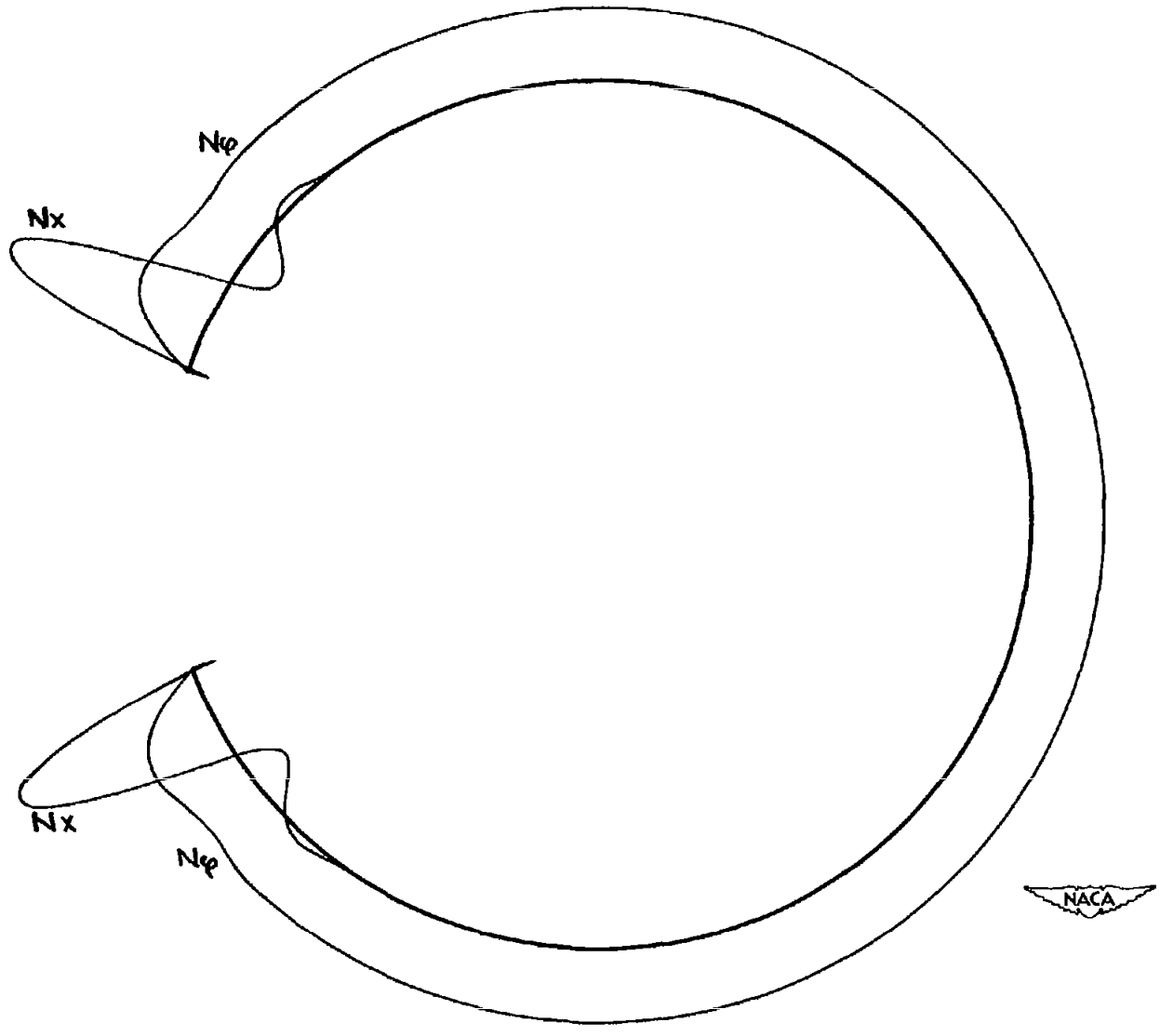

Figure 13.- Longitudinal force N_x and hoop force N_ϕ in a cross section through a cylindrical shell having a door opening.

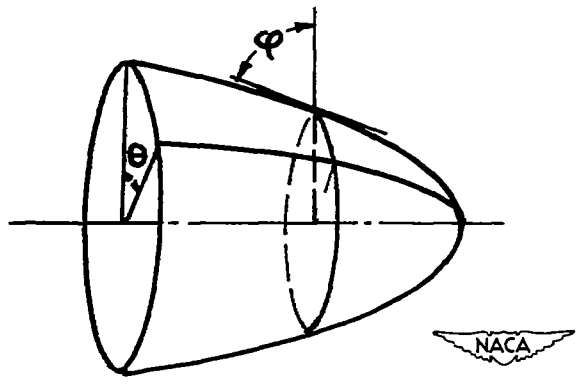

Figure 14.- Shell of revolution.

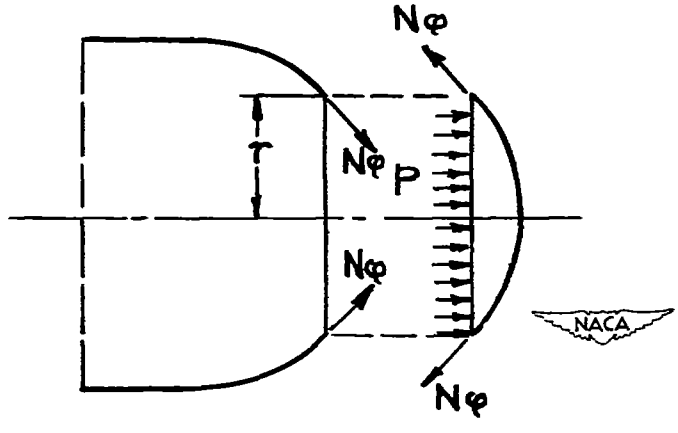

Figure 15.- Axial section through a shell of revolution.

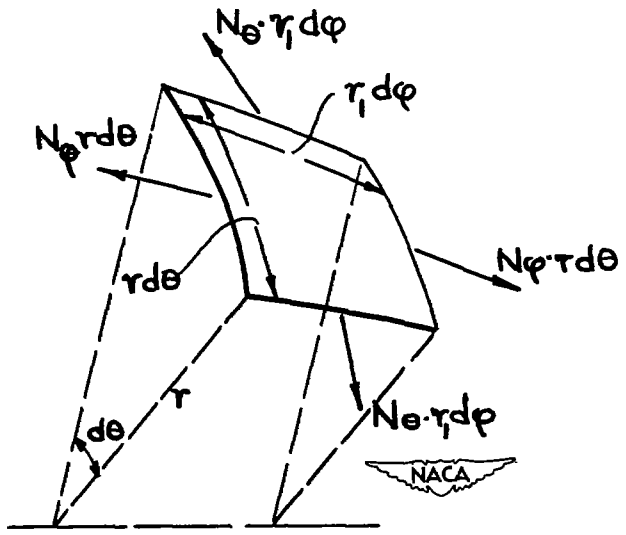

Figure 16.- Element of a shell of revolution.

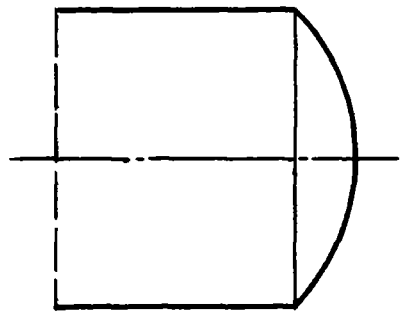

(a) Complete structure.

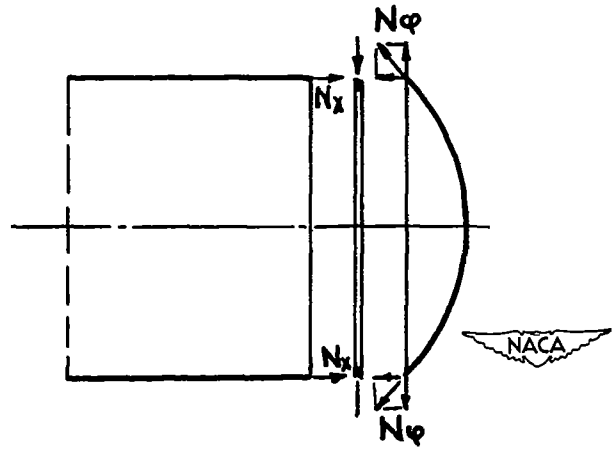

(b) Cylinder, bulkhead, and ring taken apart.

Figure 17.- Axial section through a cylindrical shell and a bulkhead.

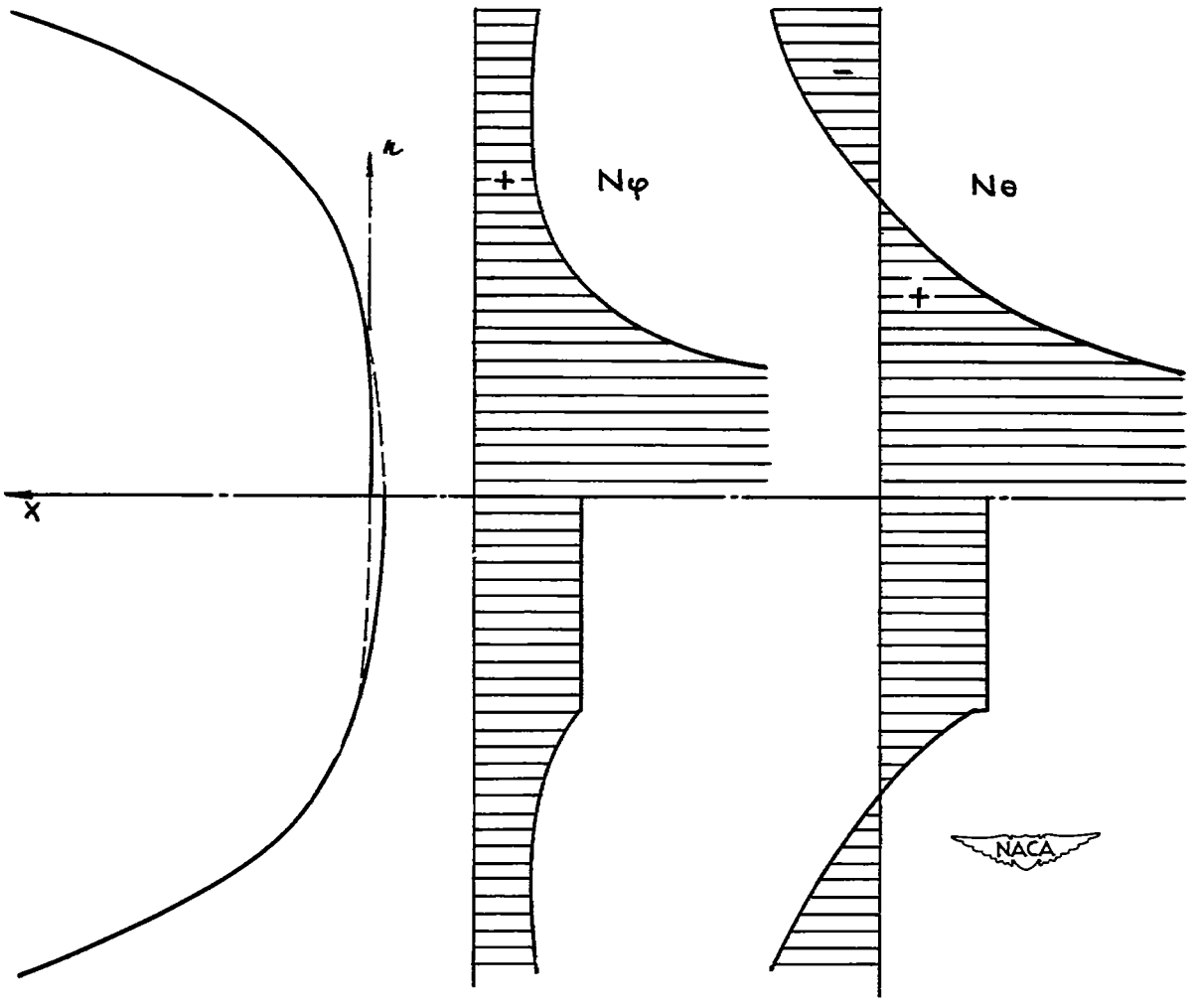

Figure 18.- Meridional force N_{ϕ} and hoop force N_{θ} in two different bulkheads. Upper half, extremely flat shape; lower half, sufficiently dished shape.

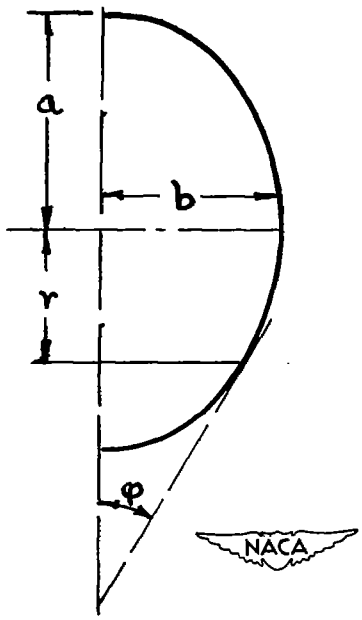

Figure 19.- Notation for an elliptic meridian.

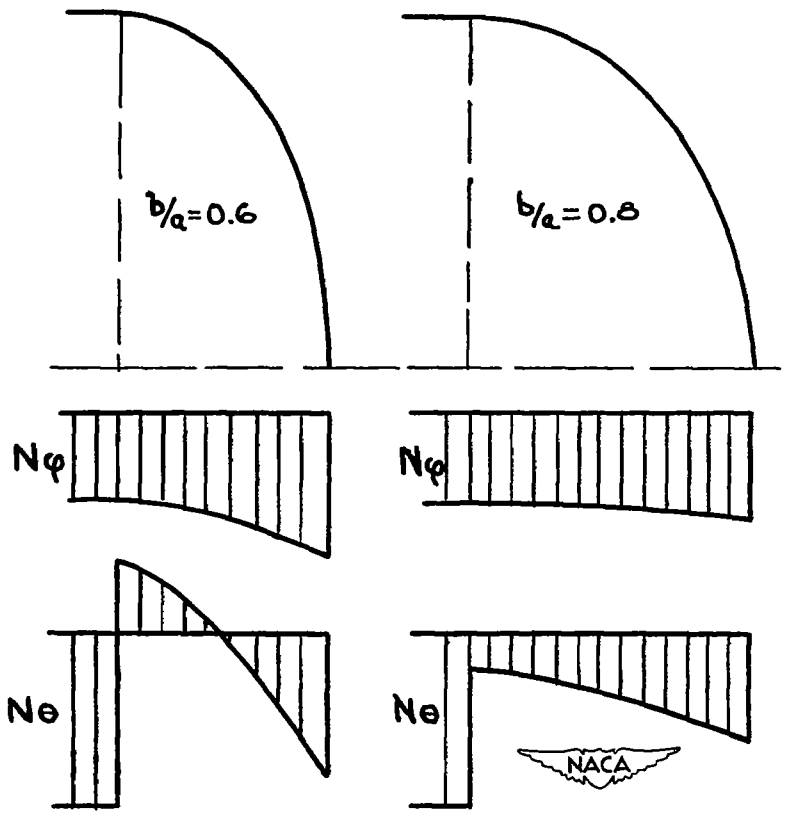

Figure 20.- Meridional force N_{ϕ} and hoop force N_{θ} in two ellipsoidal bulkheads.

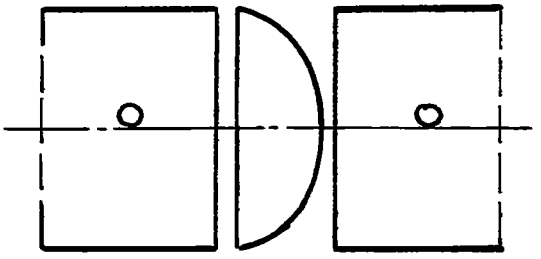

(a) Parts before pressure is applied.

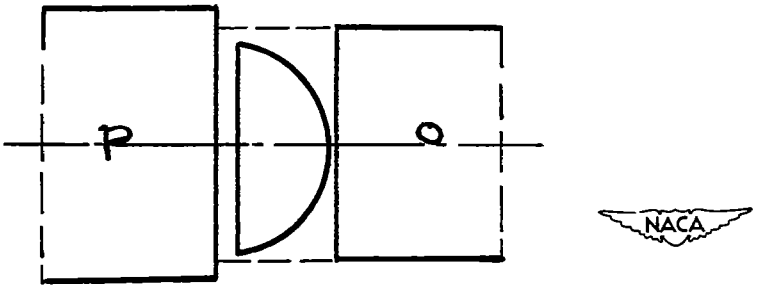

(b) Exaggerated scheme of deformation when pressure p is applied to cabin at left of bulkhead.

Figure 21.- Continuous cylindrical shell having an inserted bulkhead.

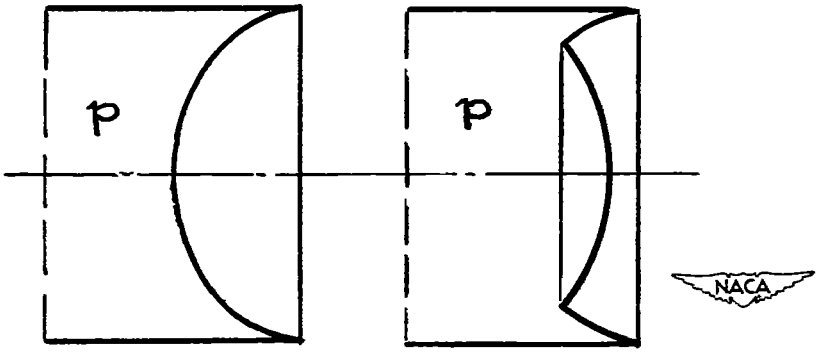

Figure 22.- Possible shapes of bulkheads.

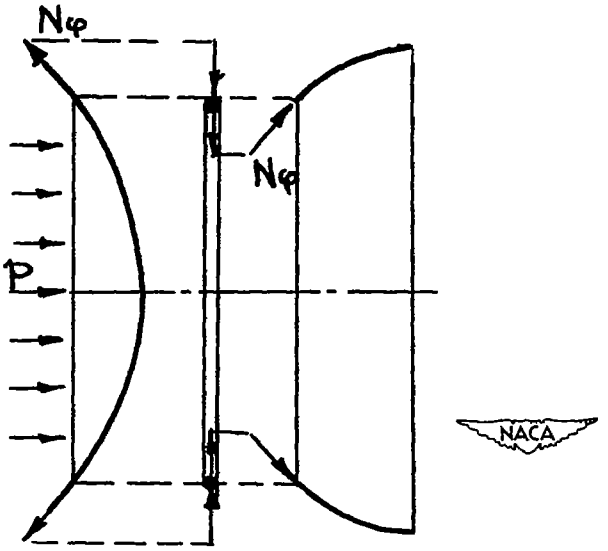

Figure 23.- Forces between parts of the bulkhead shown in right-hand sketch of figure 22.

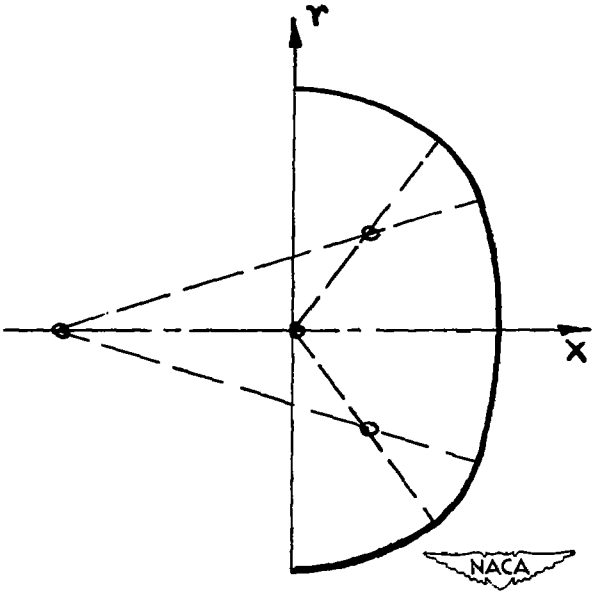

Figure 24.- Meridian of a bulkhead, built up from circles.

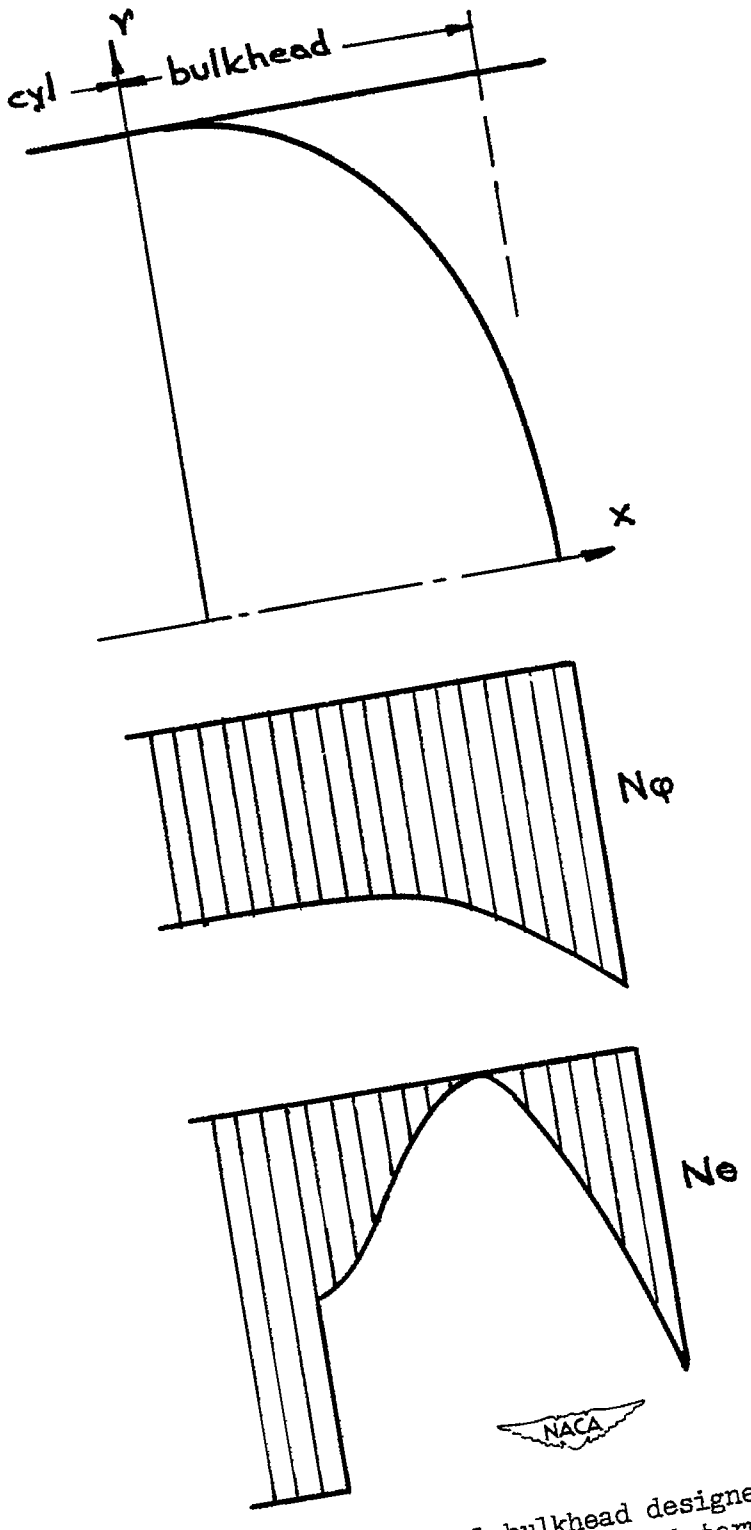

Figure 25.- Meridian of a special bulkhead designed for minimum discrepancy in membrane deformation; distribution of internal forces in this shell and in adjoining cylinder.

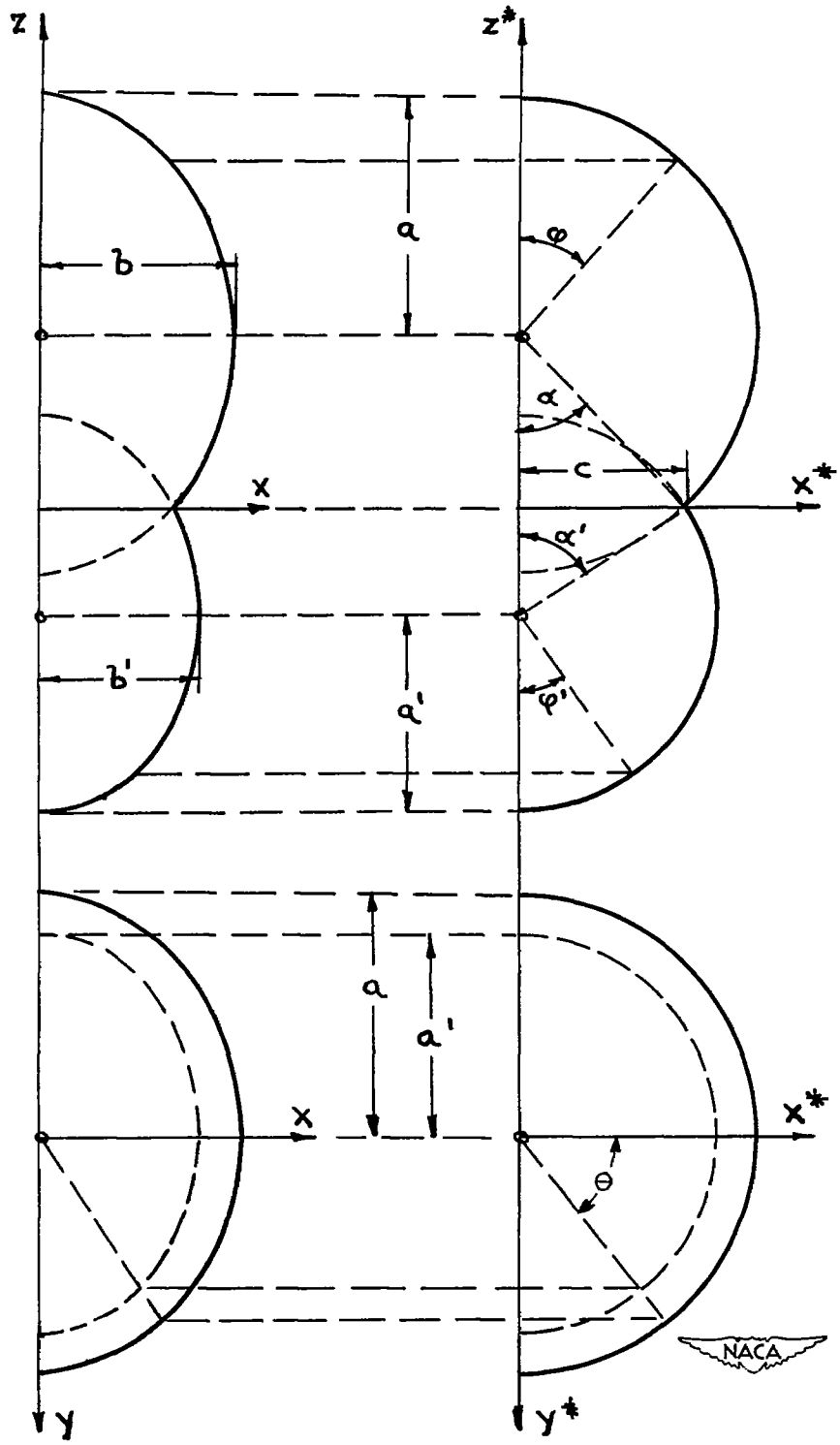

Figure 26.- Bulkhead for double cylinders, consisting of two ellipsoids (left), and corresponding spheres (right).

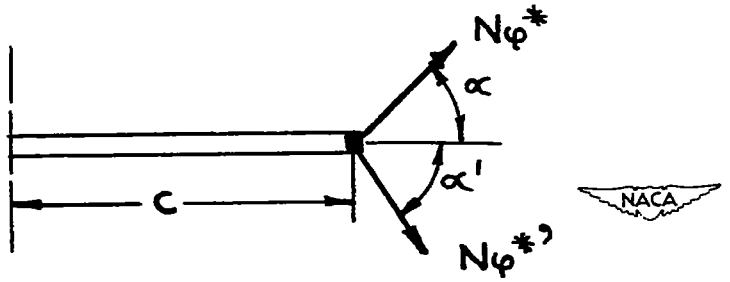

Figure 27.- Forces acting on the ring between two spheres shown in figure 26.

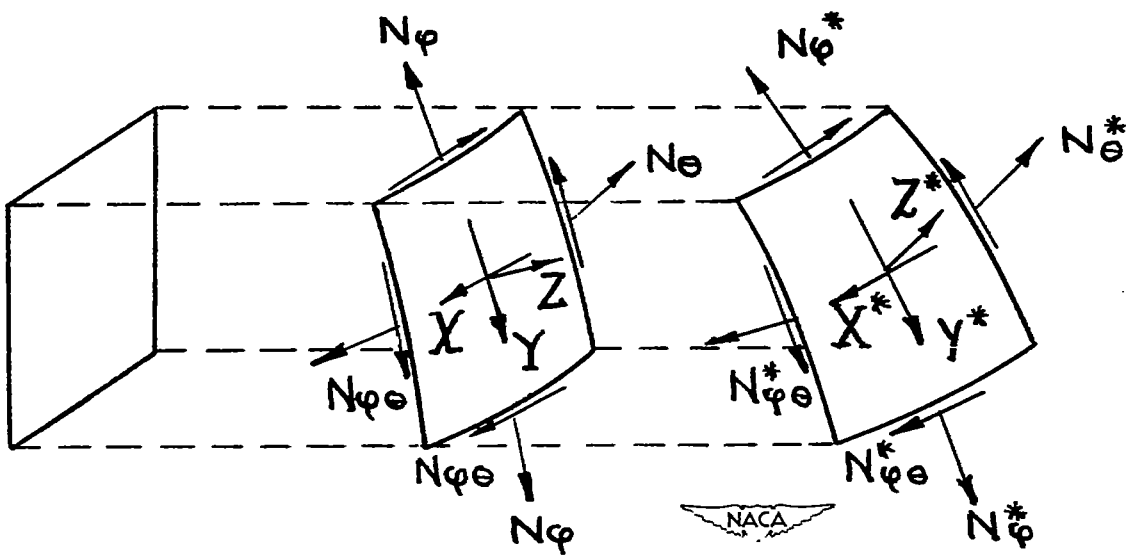

Figure 28.- Affine shell elements.

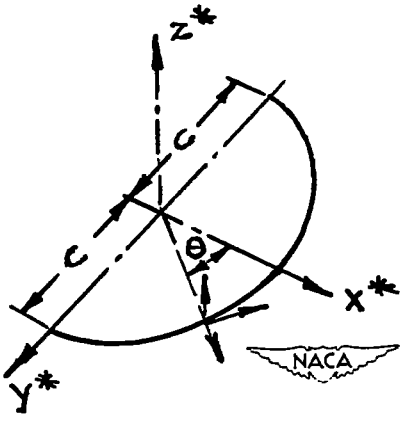

Figure 29.- Sign convention for forces transmitted from spherical shells to connecting ring.

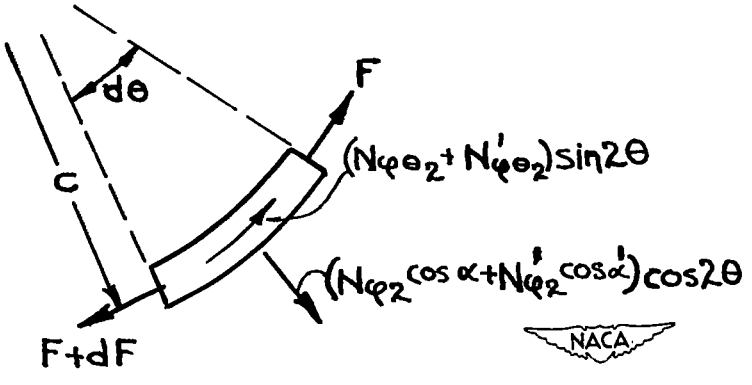

Figure 30.- Element of ring shown in figure 29.

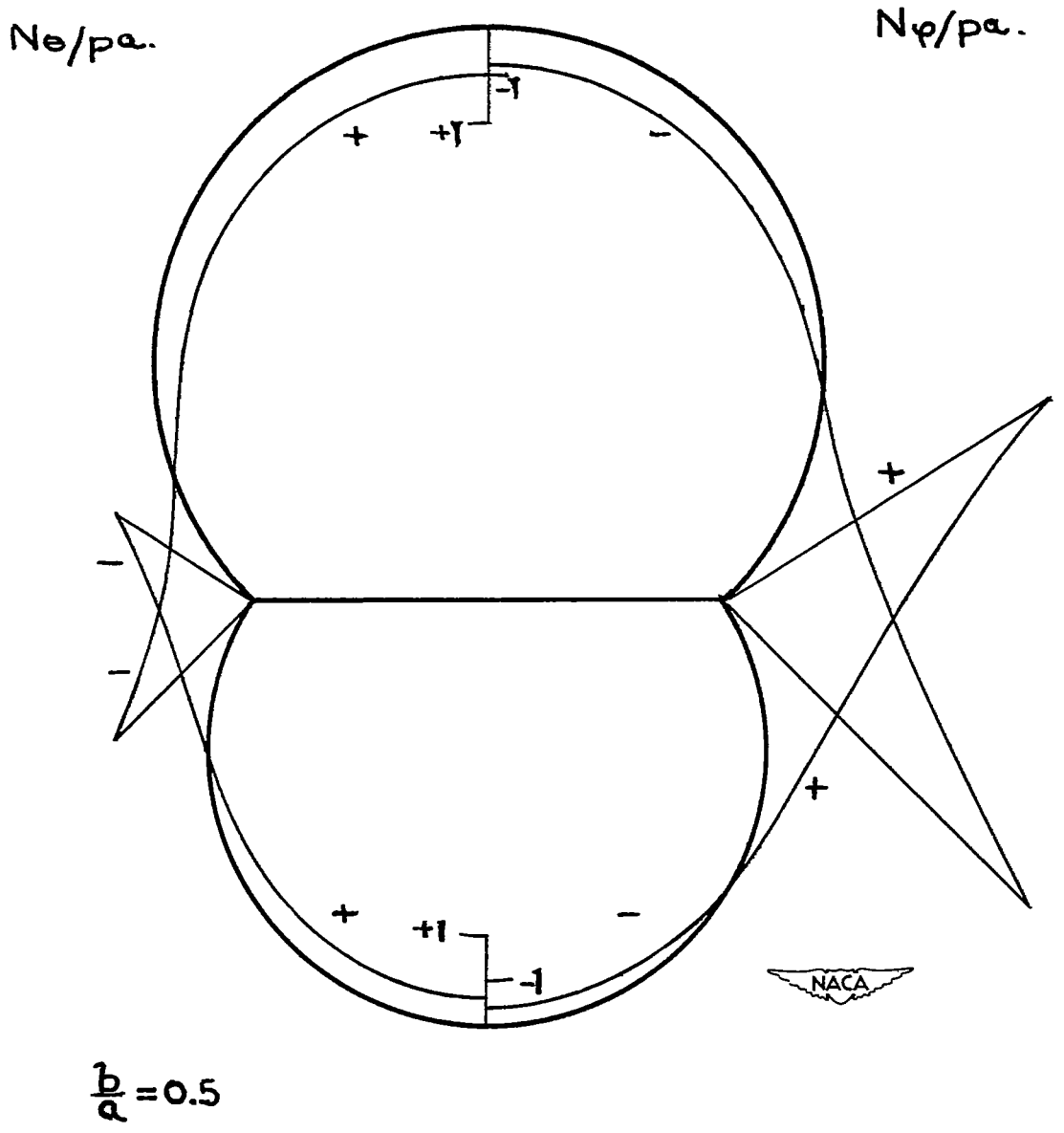

Figure 31.- Distribution of circumferential force N_θ and normal force N_ϕ at edge of ellipsoidal bulkhead shown in left half of figure 26.

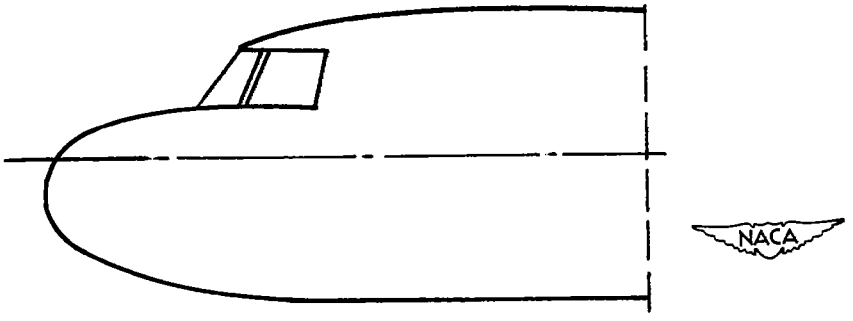

Figure 32.- Nose of a pressurized cabin.

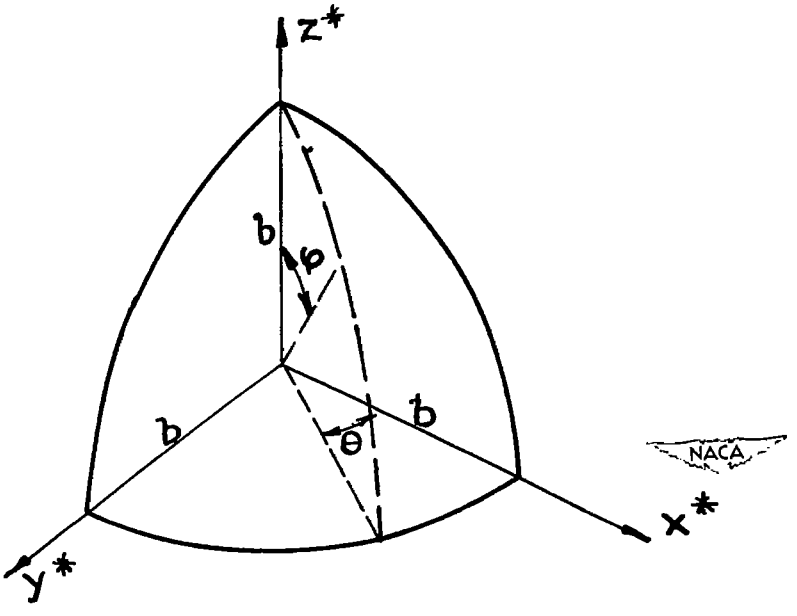

(a) Spherical shell.

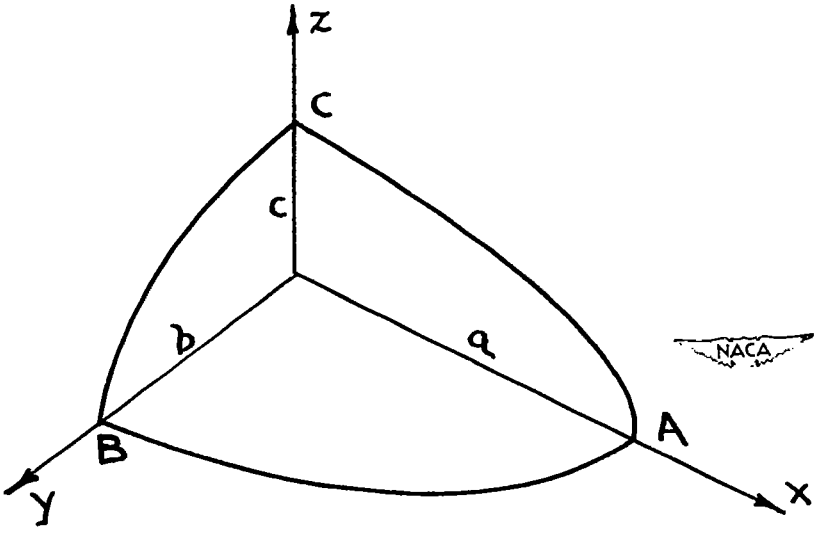

(b) Ellipsoidal shell.

Figure 33.- Sketches of shells.

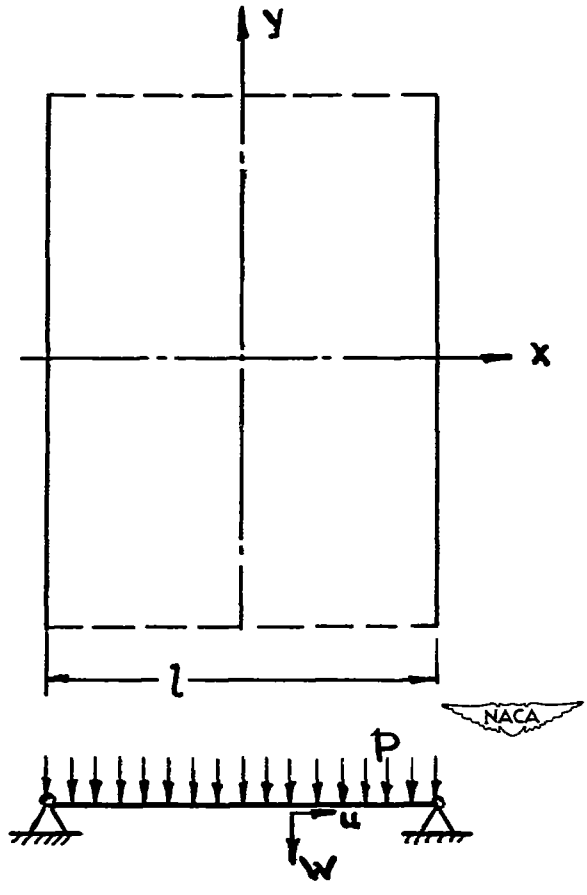

Figure 34.- Plate strip subjected to lateral pressure.

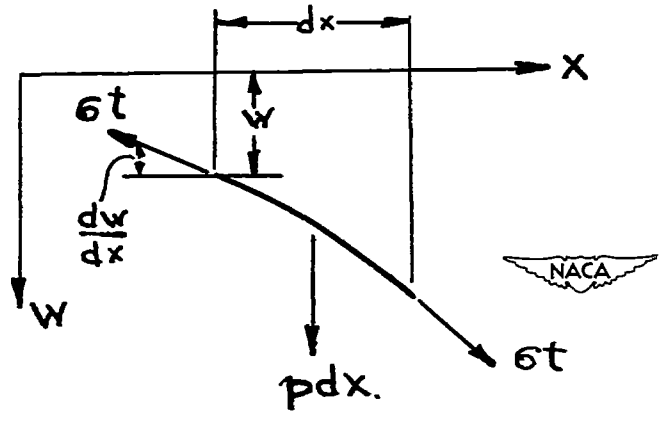

Figure 35.- Side view of an element of a plate strip.

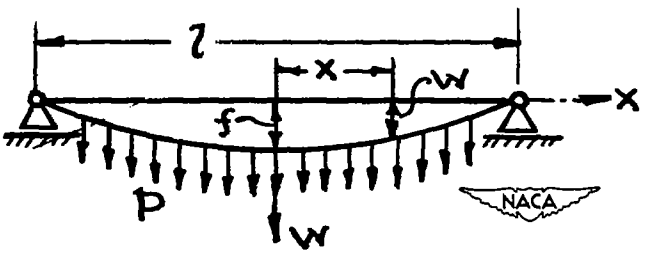

Figure 36.- Plate strip undergoing large deflection and straight stiffener.

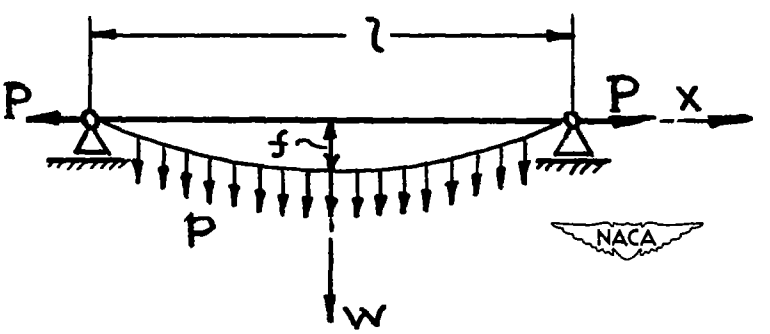

Figure 37.- Same system as in figure 36, but subjected to an additional horizontal load.

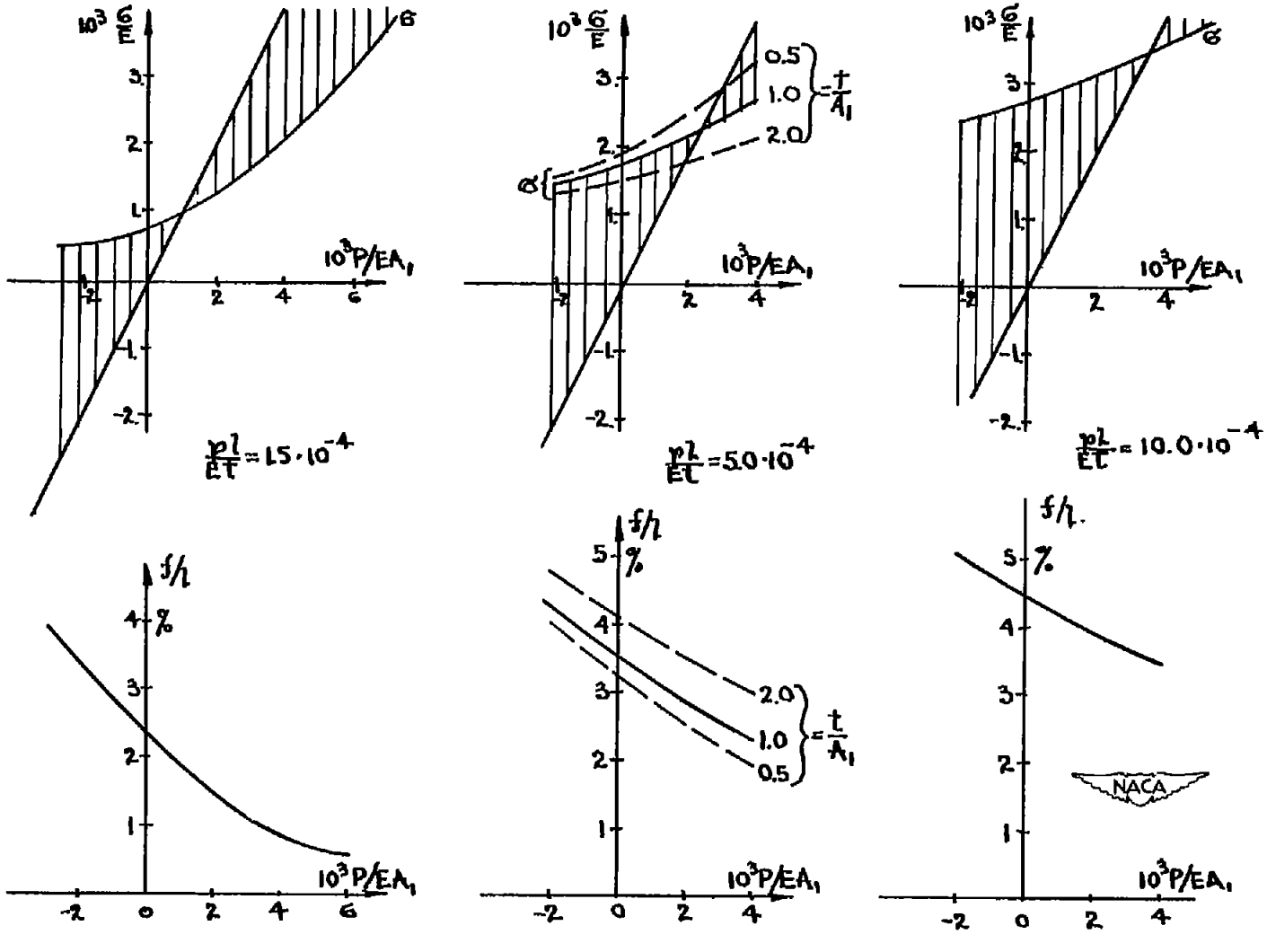

Figure 38.- Stress and deflection of plate strip, plotted against axial load, for three different lateral loads and (in central figure) for three ratios of skin to stiffener.

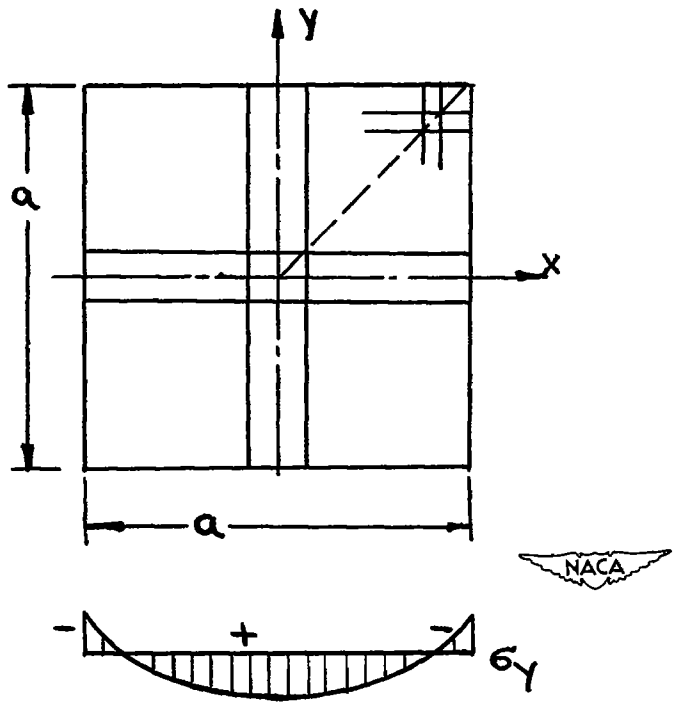

Figure 39.- Two-dimensional problem of plate with large deflection.

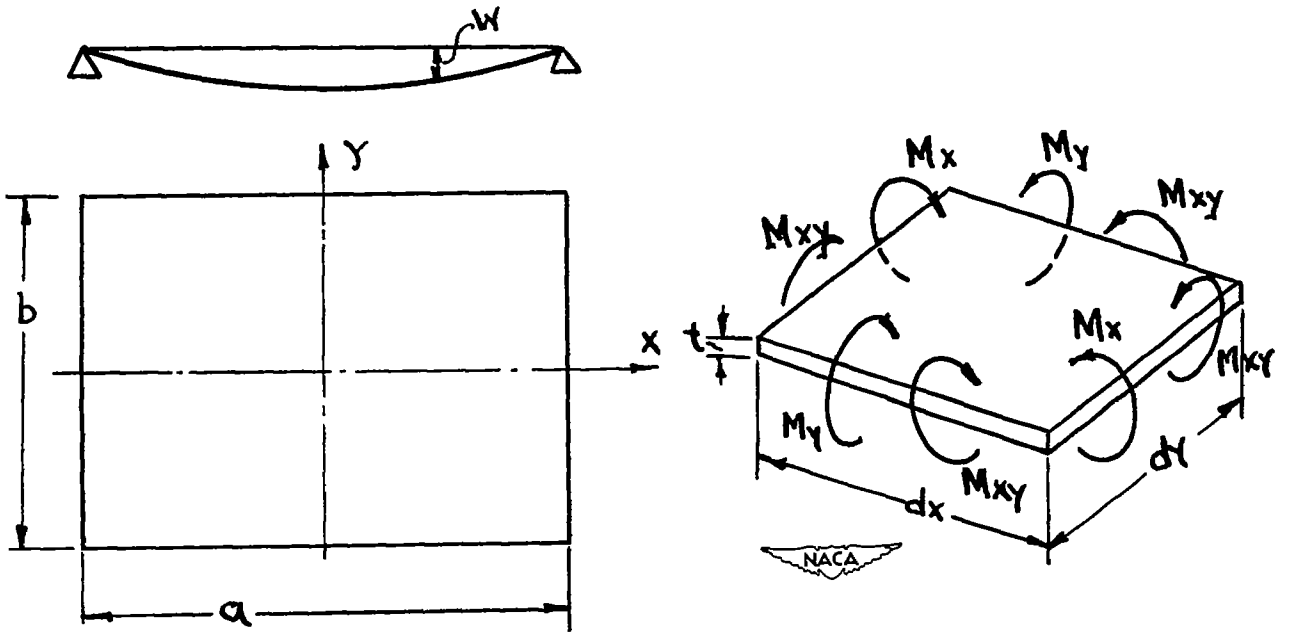

Figure 40.- Rectangular plate and plate element.

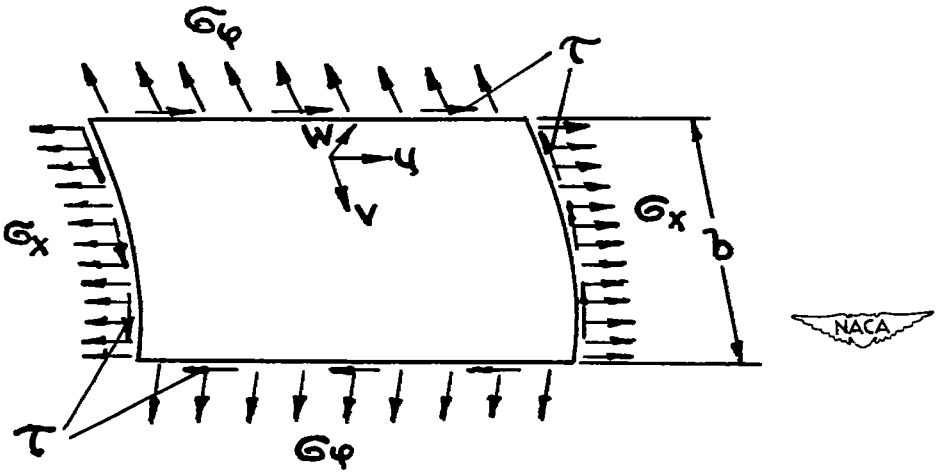

Figure 41.- Cylindrical panel.

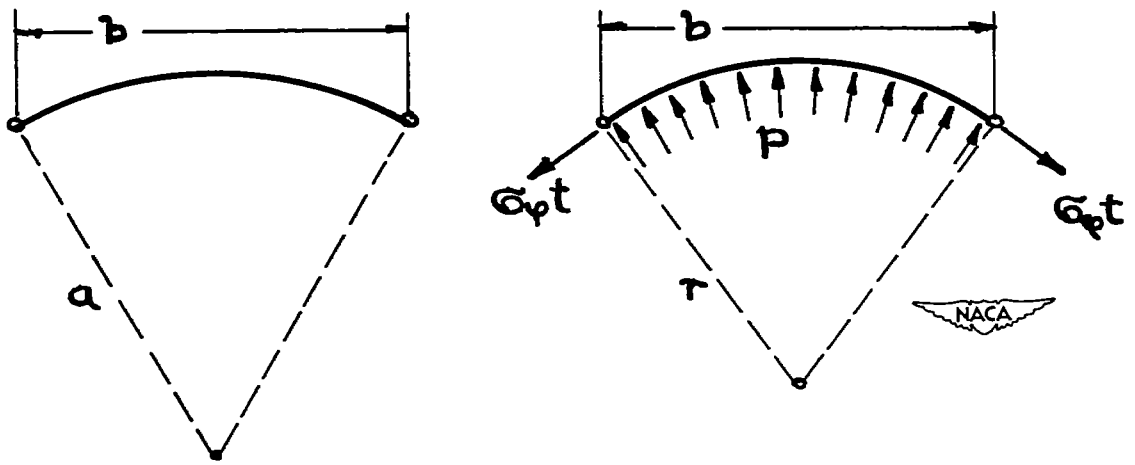

Figure 42.- Section through cylindrical panel before and after application of internal pressure p.

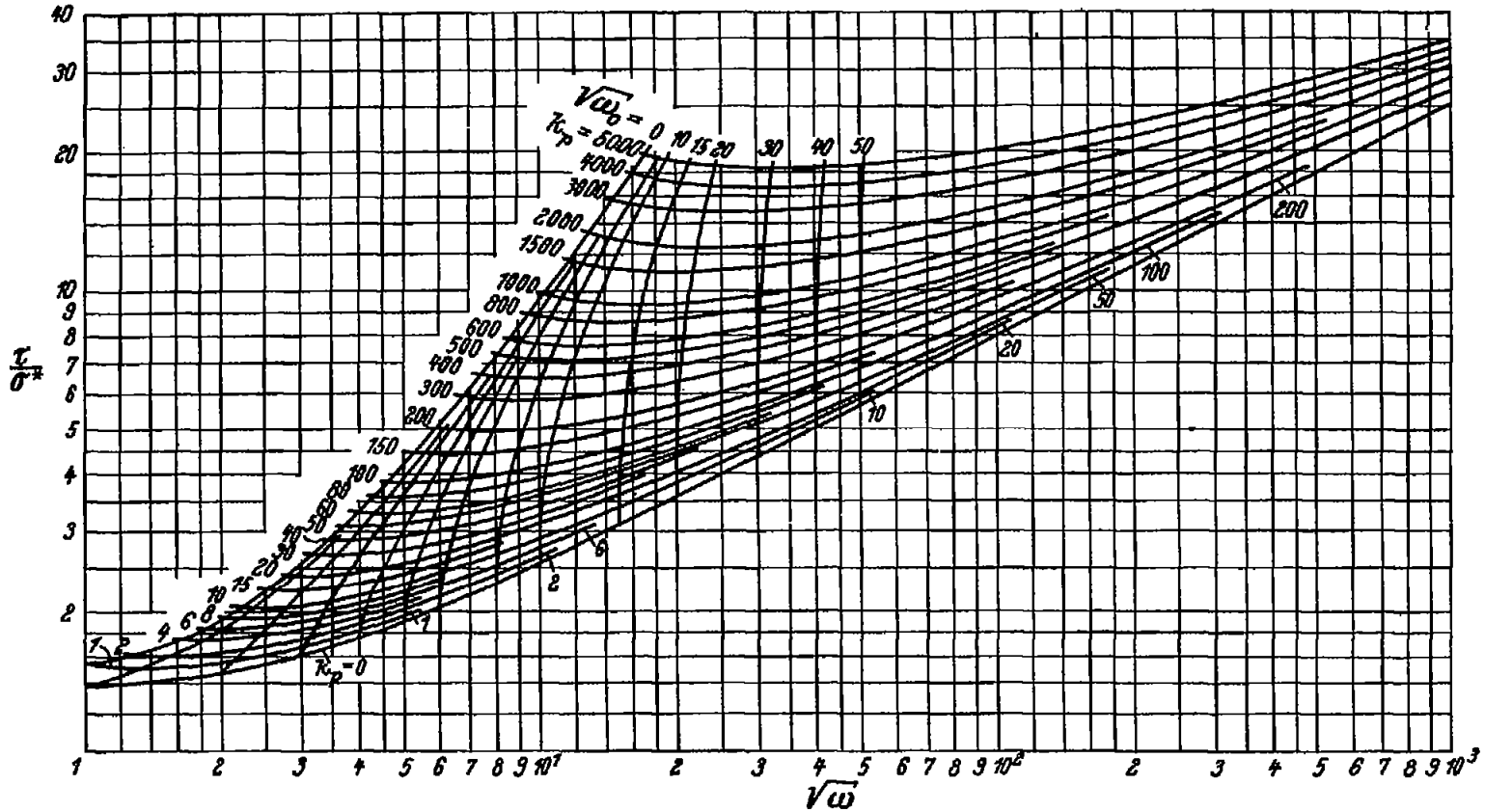

(a) $\sigma_x = 0$.

Figure 43.- Diagrams from reference 7 for buckling load of cylindrical panel shown in figure 41.

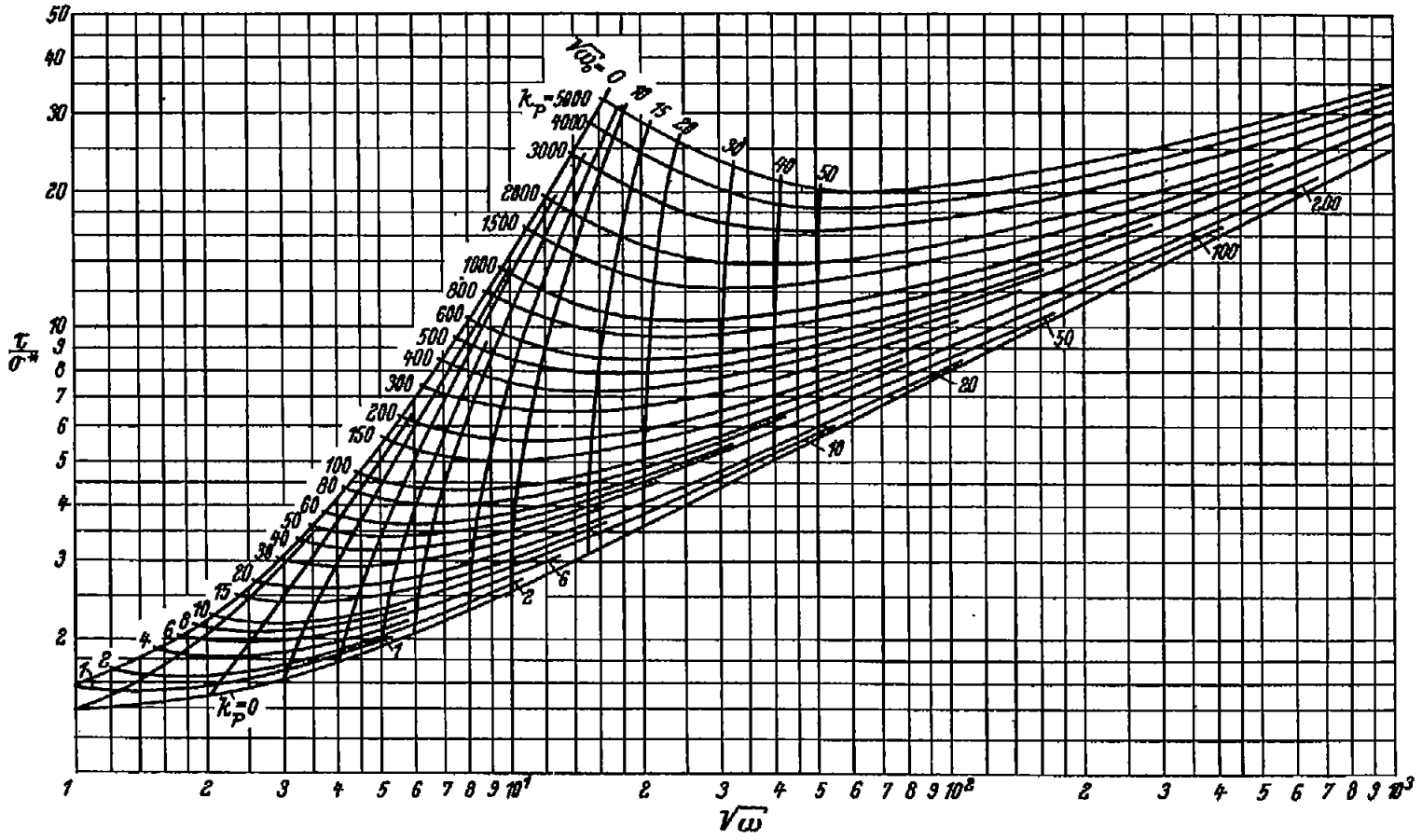

(b) $\sigma_x = \sigma_\phi/2$.

Figure 43.- Concluded.